JGR Atmospheres

RESEARCH ARTICLE
10.1029/2023JD040413

Regimes of Precipitation Change Over Europe and the Mediterranean

Julie André[1,2], Fabio D'Andrea[1], Philippe Drobinski[1], and Caroline Muller[3]

[1]Laboratoire de Météorologie Dynamique / Institut Pierre Simon Laplace, ENS—PSL Université, Ecole Polytechnique—Institut Polytechnique de Paris, Sorbonne Université, CNRS, Paris, France, [2]Ecole des Ponts, Champs sur Marne, France, [3]Institute of Science and Technology Austria, Vienna, Austria

Key Points:

- Four regimes of change for daily precipitation distribution are identified, and are captured by a two parameters analytical model
- In northern Europe, a signal of increasing mean and extreme precipitation has emerged
- In the Mediterranean, the changes of precipitation appears dominated by changes in dry-days frequency

Correspondence to:

J. André,
julie.andre@lmd.ipsl.fr

Citation:

André, J., D'Andrea, F., Drobinski, P., & Muller, C. (2024). Regimes of precipitation change over Europe and the Mediterranean. *Journal of Geophysical Research: Atmospheres*, *129*, e2023JD040413. https://doi.org/10.1029/2023JD040413

Received 9 NOV 2023
Accepted 23 JUL 2024

Abstract The Mediterranean region is experiencing pronounced aridification and in certain areas higher occurrence of intense precipitation. In this work, we analyze the evolution of the precipitation probability distribution in terms of precipitating days (or "wet-days") and all-days quantile trends, in Europe and the Mediterranean, using the ERA5 reanalysis. Looking at the form of wet-days quantile trends curves, we identify four regimes. Two are predominant: in most of northern Europe the precipitation quantiles all intensify, while in the Mediterranean the low-medium quantiles are mostly decreasing as extremes intensify or decrease. The wet-days distribution is then modeled by a Weibull law with two parameters, whose changes capture the four regimes. Assessing the significance of the parameters' changes over 1950–2020 shows that a signal on wet-days distribution has already emerged in northern Europe (where the distribution shifts to more intense precipitation), but not yet in the Mediterranean, where the natural variability is stronger. We extend the results by describing the all-days distribution change as the wet-days' change plus a contribution from the dry-days frequency change, and study their relative contribution. In northern Europe, the wet-days distribution change is the dominant driver, and the contribution of dry-days frequency change can be neglected for wet-days percentiles above about 50%. In the Mediterranean, however, the change of precipitation distribution comes from the significant increase of dry-days frequency instead of an intensity change during wet-days. Therefore, in the Mediterranean the increase of dry-days frequency is crucial for all-days trends, even for heavy precipitation.

Plain Language Summary The Mediterranean region is facing increased dryness alongside more intense rainfall in certain areas. We delved into the change of precipitation frequency and intensity across Europe and the Mediterranean using ERA5 reanalysis data from 1950 to 2020. Our analysis revealed four distinct patterns in how rainfall is evolving. In much of northern Europe, heavy rainfall events are becoming more frequent, while in the Mediterranean, lighter precipitation is decreasing while heavy rain is either increasing or decreasing. To understand these changes better, we used a mathematical model with two parameters. This model helped us track the types of changes in precipitation patterns. We found that in northern Europe, the increase in rainfall intensity is the primary driver of change, while in the Mediterranean, it's more about the increase of the dry-days frequency. These findings underscore the importance of considering both the frequency and intensity of precipitation when studying climate change impacts. By understanding these shifts, we can better prepare for future weather extremes in these regions and adapt to the changing climate.

1. Introduction

Climate change is known to impact the global water cycle, and to have consequences on total precipitation and extreme of precipitation. The changes expected on total precipitation are of about +2%−3% per degree Celsius of global warming, while for the extreme precipitation, estimates from thermodynamics give at first order a rise in intensity of about 7%/°C (Allen & Ingram, 2002; Held & Soden, 2006; Trenberth, 1999). However, on regional scales the changes in mean and extreme precipitation can vary substantially from the global mean, due both to dynamical aspects and natural variability (Fischer et al., 2013; Fischer & Knutti, 2014; Pendergrass & Hartmann, 2014; Pfahl et al., 2017; Trenberth, 2011).

The Mediterranean region, due to its unique position as a transition zone between the wetter Europe and the dryer desert of the Sahara, is a climate change hotspot in terms of temperature and precipitation changes (Giorgi, 2006; Urdiales-Flores et al., 2023). Climate projections predict that the Mediterranean will get drier (more evaporation and decreased mean precipitation) with global warming (D'Agostino & Lionello, 2020; Drobinski et al., 2020) and will experience more extreme precipitation, at least on the northern shore (Ali et al., 2022; Drobinski

et al., 2018; Giorgi et al., 2014; Myhre et al., 2019; Pichelli et al., 2021; Vautard et al., 2014). This simultaneous decrease in mean precipitation and increase in extreme precipitation is sometimes called a "paradox in the water cycle change" (Alpert et al., 2002; Brunetti et al., 2000; Brunetti et al., 2004; Zittis et al., 2021). Northern western and central Europe, on the contrary, are expected to undergo an increase of both total precipitation and extreme precipitation (Zittis et al., 2021; Intergovernmental Panel On Climate Change, 2023, chapter 8).

Still, the long-term water cycle changes in the Mediterranean are unclear when looking at historical observations. In past data, previous studies find a strong and significant signature of increasing evaporation and of drier conditions, such as droughts or dry spells (Caloiero et al., 2018; Hoerling et al., 2012; Raymond et al., 2016; Sheffield & Wood, 2012), associated to an increase of dry-days frequency over the Mediterranean and a decrease over Europe (Benestad et al., 2019; Brunetti et al., 2000; Brunetti et al., 2004), but the trends of the mean precipitation are subject to more debate. The 6th Intergovernmental Panel on Climate Change (IPCC) assessment report (Intergovernmental Panel On Climate Change, 2023, chapter 8) concludes that there is no long-term trend of the mean precipitation in the Mediterranean since the pre-industrial era. Only on shorter time periods of the order of a few decades or on sub-regions can some significant trends be derived (Azzopardi et al., 2020; Mariotti et al., 2015; Sousa et al., 2011; Tanarhte et al., 2012; Zittis, 2018), but they may be driven mainly by natural variability and not by climate change (Peña-Angulo et al., 2020).

In this paper, we want to study the whole precipitation distribution over the Mediterranean region. Compared to droughts and extreme precipitation, which have been extensively studied, the research on the whole precipitation distribution is relatively less developed. In the few papers that do study the whole range of the precipitation distribution, two main approaches can be distinguished: non-parametric and parametric studies. Non-parametric studies focus on the changes of frequency of fixed precipitation intensity amounts or on the changes of intensity for fixed percentile ranks or on the change of contribution from given precipitation amounts to the total precipitation (Alpert et al., 2002; Berthou et al., 2019, 2020; Brunetti et al., 2004; Klingaman et al., 2017). These methods are interesting, but when one wants to allow diagnostics or interpretation in terms of a few key parameters, parametric studies are needed.

Still, very few parametric studies consider the whole precipitation distribution and do not focus only on extreme precipitation. One of these few studies took a simple exponential law with a single parameter (Benestad et al., 2019) while another study took a gamma law, which was shown to perform quite well for the low to medium precipitation (Ben-Gai et al., 1998; Groisman et al., 1999). A more complex model, tailored for wet-days precipitation, has been recently proposed by Naveau et al. (2016) and gives very good results for both the low precipitation and the extremes (Rivoire et al., 2022; Tencaliec et al., 2020), still with a little more complexity (it has three parameters compared to two for the gamma law or one for the exponential). In this paper, we choose the intermediate approach of a Weibull law with two parameters, which, as will be shown below, represents a minimal framework to model wet-days distribution and its quantile trends regimes.

In this work, we propose a framework which describes the change over time of the whole distribution of precipitation: from absence of precipitation to low and moderate precipitation, up to extreme events. We first perform a description of the wet-days trends, quantile by quantile. As underlined by Schär et al. (2016), such a method should consider the change in frequency of non-precipitating days (or "dry-days"). Therefore, we also study how the wet-days quantile trends can be influenced by the change in dry-days frequency. We illustrate this methodological framework on the recent past in Europe and the Mediterranean. The main question addressed here is the following: how does the whole precipitation distribution change across Europe and the Mediterranean region?

The outline of the paper is as follows: Section 2 presents the data set used, then Section 3 presents the different kinds of regimes that can be observed over Europe and the Mediterranean concerning the wet-days quantile trends. Section 4 proposes the Weibull law as a wet-days distribution to represent the observed regimes, and analyze them more thoroughly. Section 5 extends this parametric model to the all-days distribution, with an application on the trends of the total precipitation and of all-days quantiles.

2. Precipitation Data Set

We chose to use a single data set in this study to focus on the development of a methodological framework. Yet, we would like to highlight that the methodology we present in this paper can be applied to any other precipitation data sets.

The choice of the data set was driven by the need for a data covering the whole Euro-Mediterranean region, with spatially and temporally homogeneous precipitation, as well as covering a period of time long enough to help detect small changes in the precipitation distribution out of the natural variability.

We used ERA5 reanalysis, the latest global reanalysis provided by the European Center for Medium-Range Weather Forecasts (Hersbach et al., 2020) at a resolution of 0.25°, on the period 1950–2020. We computed the daily accumulated precipitation from ERA5 hourly variable "total precipitation", which incorporates both convective and large-scale precipitation. Our domain covers the area between 25°W and 45°E in longitude, and between 25°N and 71°N in latitude, enabling the study of both the Mediterranean and Europe.

ERA5 assimilates observations which constrain properties like large scale moisture convergence, and the model is run at an improved resolution compared to the previous version, ERA-Interim. Thus it has been argued that ERA5 shows reduced uncertainty in its representation of the convective environment (Taszarek, Allen, et al., 2021; Taszarek, Pilguj, et al., 2021) and of heavy precipitation (Chinita et al., 2021). ERA5 reanalysis has been shown to be of very good quality on the pan-European domain, with a wet-days frequency spatial pattern well represented, though it overestimates this frequency, by about 10%–20% over land, and thus the mean precipitation (Bandhauer et al., 2022; Rivoire et al., 2021). ERA5 wet-days precipitation intensity has been shown to be in very good agreement with the reference European station-based gridded data set E-OBS (Cornes et al., 2018) over European lands, especially where E-OBS is most trusted, that is, where its station density is high (especially in Germany, Ireland, Sweden, and Finland).

As our results are derived from ERA5 reanalysis only, we are aware of potential temporal inhomogeneities in the precipitation data: trends might be susceptible to time-dependent biases, for example, due to the change of assimilated observations in the reanalysis. Yet, temporal inhomogenities in reanalyses have been mainly noticed in region with sparse data, such as Africa and more generally the southern hemisphere (Ambrosino & Chandler, 2013; Kistler et al., 2001), usually due to the addition of satellite data (e.g., Krueger et al., 2013 on storms, or Shangguan et al., 2019 on ozone data), or to an increase in station density mainly before the 1950s (Ferguson & Villarini, 2012; Pohlmann & Greatbatch, 2006). Therefore, we expect the ERA5 data in Europe and the Mediterranean to be much less prone to temporal inhomogenities. Besides, we compared trends in precipitation standard deviation in ERA5 and in E-OBS gridded data set, and while we noticed strong temporal biases on E-OBS—with very strong non-physical differences between neighbor countries—such biases were not visible at all in ERA5 precipitation data.

3. Observed Regimes for the Change of the Wet-Days Distribution

One way to study the changes of distribution of precipitation is to look at the evolution of the cumulative distribution function, or equivalently its inverse function, the quantile curve, on which we will focus in this study. In the following, we designate as trend the absolute change of a given variable between two periods of 31 years, 1950–1980 and 1990–2020. We choose to take periods of three decades to smooth out the natural variability within those periods when taking the mean statistics. The impact of the choice of the dates on our results is negligible (see Appendix A). To study the evolution of the quantile curve with time, we thus computed the trends between the quantile curves of the two time periods: we thus obtain the curve of the intensity change for each wet-days percentiles.

A precipitation distribution usually has a high probability of the event 0 mm, corresponding to the many dry-days, that is, days with no to very low precipitation accumulation. In this paper, we will look at both the change of precipitation occurrence and intensity of precipitation (i.e., wet-days distribution) but also the all-days distribution. For methodological issues, it is indeed handy to set aside the dry-days and fit a model on the wet-days distribution only (which will be done in the next section). We are conscious that a quantile trend defined on a wet-days distribution may be influenced by a change in the frequency of dry-days, f_d, as discussed in detail in Schär et al. (2016): this aspect will be further developed in Section 5.

We followed the work from Expert Team on Climate Change Detection and Indices, which recommends the use of 1 mm/day as the threshold for the definition of dry and wet-days. This value enables to better deal with both the issues of under-reporting of small precipitation amounts in observations and the "drizzle problem" of models and reanalyses—which usually have too many days with weak precipitation (Karl et al., 1999; Zhang et al., 2011). The

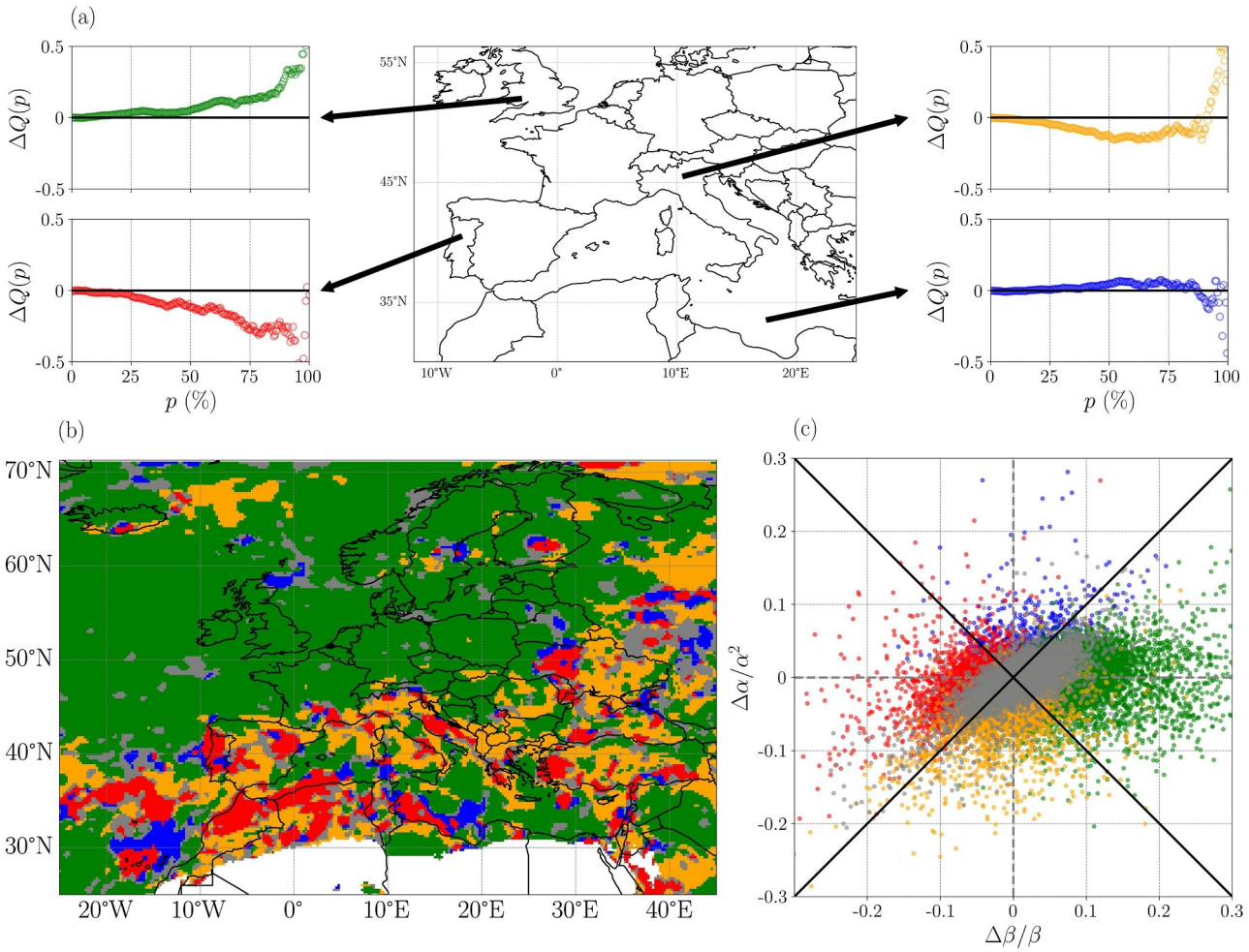

Figure 1. (a) Illustration of the four types of behaviors for wet-days quantile trend curve (between 1950–1980 and 1990–2020), at four chosen locations. The quantile trends $\Delta Q(p)$ are plotted in mm/day/decades. (b) Wet-days category map obtained from the classification algorithm, applied on the trends between 1950–1980 and 1990–2020, with a sliding window of nine grid-points. Green corresponds to "nearly all quantiles intensify" category, red to "nearly all quantiles decrease", orange to "U-shape" and blue to "reversed U-shape." Gray means the category is unclear. White designates desert location (less than 2% of wet-days). (c) Relative change of Weibull parameters $\left(\frac{\Delta\beta}{\beta}, \frac{\Delta\alpha}{\alpha^2}\right)$ for the wet-days precipitation distribution, plotted for the whole domain. This Weibull model is defined in 4. Colors indicate as before the category detected by the classification algorithm. The black thick lines are the theoretic limits between the influence zones of the two Weibull parameters.

frequency of dry-days (days with less than 1 mm/day) is far from being negligible in our domain, and can vary from 20% in northern Europe up to 90% in the Maghreb (and almost 100% in the desert).

We illustrate in Figure 1a the four main qualitatively different regimes which can be found on the domain, depending on the shape of the wet-days precipitation quantiles trend curve:

- a regime where nearly all quantiles intensify (for ex. in the UK),
- a regime where nearly all quantiles decrease (for ex. in the North of Portugal, although a few of the most extremes may have a slightly positive trend),
- a U-shape regime, consisting in negative trends for low to medium quantiles but positive trends on extremes, with a certain inversion percentile in between (for ex. in the North of Italy),
- a reversed U-shape regime, with increasing low to medium percentiles with decreasing extremes (for ex. in the Mediterranean Sea just North of Libyan coast).

Note that by construction, the trend of the 0% wet-days percentile will always be zero, as its intensity is by definition fixed to 1 mm/day.

Note that a regime comparable to this "U-shape", with a "crossover" or "inversion percentile", was already mentioned in literature for the Mediterranean region (Boberg et al., 2010; Colin, 2011).

In order to quantitatively distinguish between those regimes of trends, we developed a simple classification algorithm, which takes in input a list of percentiles and associated quantile trends, looks at the shape of the trend curve and assesses in which of the four categories it falls into. It uses the signs of the trends for both low to medium ranks (the "belly" of the curve, for percentiles $p \in [10\%, 60\%]$) as well as for extreme high ranks (the "tail" of the curve, for percentiles $p \in [85\%, 99\%]$). It also uses the slope of the linear regression for percentiles $p \in [60\%, 99\%]$.

More precisely, the algorithm is the following.

1. If the means of the belly is positive, and the tail has a positive mean and slope, then the category is defined as "all quantiles intensify."
2. If the mean of the belly is negative, but the tail has a positive mean and slope, then the category is defined as "U-shape."
3. If the mean of the belly is negative and the tail has a negative mean and slope, then the category is defined as "all quantiles decrease."
4. If the mean of the belly is positive while the tail has a negative mean and slope, then the category is defined as "reversed U-shape."

Finally, if the curve doesn't fall into any of these four categories, it is set into the "unknown" category.

This classification algorithm was applied over the whole Mediterranean and European domain, between 1950–1980 and 1990–2020, giving the category map shown in Figure 1. Note that this map was obtained by applying the algorithm on a sliding window of nine pixels (which for each grid-point merges together the quantiles trends of its eight neighboring grid-points) to smooth out very local irregularities.

The first thing that becomes manifest on the category map in Figure 1b is a clear North/South pattern: a large majority of North–West Europe as well as subtropical Atlantic Ocean belongs to the same regime ("all quantiles intensify"), while the Mediterranean region is mainly in the "U-shape" regime (i.e., decreasing low to medium quantiles but increasing extremes) with also a certain amount of "all precipitation quantiles decrease" regime. This is consistent with what one would expect from a Mediterranean type behavior, with both drying and extreme precipitation events intensification. In the southern part of the Mediterranean basin, the "all decrease" regime is more predominant. We remind that the differences between the "all-decrease" and "U-shape" categories are mainly due to their opposite trend signs for very heavy precipitation. We can also observe that for the Mediterranean Sea far from the coasts (about 200 km away), the dominant category is the "all quantiles intensify" one. As for African land equatorward of 30°N, the category map becomes extremely spotty, which could be due to a higher natural variability in the wet-days distribution, mainly due to the very small number of wet-days. Therefore, we won't look at desert regions, where there is less than 2% of wet-days.

We also note that the map of categories is much spottier within the Mediterranean region than in northern Europe. This spottiness seems to stem primarily from a strong natural variability, which may have prevented a clear long-term climate change pattern from emerging in the distribution of wet-days in the Mediterranean. Indeed, as shown in Appendix A, the agreement between wet-days category maps computed for different time periods over 1950–2020 is much lower for the Mediterranean than for northern Europe.

As a sum up, the signal of an intensification in the wet-day distribution is clear in northern Europe, while the Mediterranean region does not seem to have yet a signal strong enough to overcome the noise of natural variability. This is a motivation to try to assess more quantitatively the significance of a signal by taking a parametric approach.

4. Analytical Model for the Wet-Days Precipitation Distribution

In order to synthesize the information on each and every quantile trends into a smaller number of parameters, we turn to a parametric approach.

We first focus on finding a model for the wet-days distribution. Then in Section 5 we will see how all-days quantiles trends can be influenced by the changes of both the wet-days distribution and the dry-days frequency.

4.1. Choice of a Distribution Model

There is no standard model for precipitation's annual distribution in the literature, but different choices depending on the aim of the study and the data considered.

Benestad et al. (2019) used an exponential law for the wet-days precipitation distribution, which worked well on their observational data and gave a good "rule of thumbs" to relate extremes probability or quantile trends to the wet-days mean. However, since this wet-days model has a single parameter (the wet-days mean), it can only represent a shift of all quantiles to higher (resp. lower) intensities if the parameter increase (resp. decrease). Thus this exponential model can not represent the two other quantile trends regimes we observe, the "U-shape" and "reversed U-shape", which have opposite trends for low and high percentiles. We need at least two parameters in the wet-days distribution in order to represent the four regimes presented in 3.

We compared different models with two or three parameters, among some usually-used models for precipitation distribution (Gamma, Weibull, Lognormal, Pearson, etc.) on ERA5 precipitation data, using the maximum likelihood estimation method and two goodness-of-fit estimators (Kolmogorov-Smirnov and Cramer von Mises). See Appendix B for more details. From this comparison of the different models fitted on ERA5 precipitation data, we showed that the best model was the 3-parameters so-called Naveau distribution (Naveau et al., 2016) seconded by the 2-parameters Weibull distribution. For this study, we preferred to work with the Weibull distribution, as its two parameters are already sufficient to describe the four quantiles regimes, as we show in the following.

4.2. Expression of the Four Regimes Through a Weibull Model

A Weibull distribution is defined by two parameters: a shape parameter (called α) and a scale parameter (called β). The cumulative distribution function of a Weibull law is expressed as:

$$g(x) = 1 - e^{-(x/\beta)^{\alpha}}$$

where x is the intensity of precipitation ($x > 1$ mm/day by definition of wet-days), and $g(x) = p \in [0, 1]$ is the probability of having a wet-day with a precipitation inferior or equal to x. Note that p is also the percentile rank corresponding to an event of precipitation intensity x. Note that α and β are both positive, and $\alpha \leq 1$. The scale parameter β can be thought of as representative of the distribution median and has a unit of mm/day, while the shape parameter α is linked to the precipitation variance (though it is dimensionless). For a given percentile p, the quantile intensity $Q(p)$ in mm/day is obtained as the inverse of the cumulative distribution function:

$$Q(p) = x = \beta\left[\ln\left(\frac{1}{1-p}\right)\right]^{1/\alpha} \tag{1}$$

In Equation 1 it becomes clear that β is also the intensity of the quantile of rank $p = 1 - e^{-1} \approx 0.63$, giving $\beta \approx Q(63\%)$. We can thus think of the scale parameter β as (quite close to) the wet-days precipitation median. We finally note that when $\alpha \to 1$, the Weibull model simplifies to an exponential distribution, giving the same expressions as in Benestad et al. (2019), with the parameter β becoming the wet-days mean. The values of the Weibull parameters for ERA5 precipitation data are provided in Appendix C, as well as their trends and the fit uncertainties.

Quantile trend curves like the ones shown in Figure 1 can be expressed analytically as $\Delta Q(p)$, Δ denoting the change between two periods of time (denoted by the subscripts 1 and 2):

$$\Delta Q(p) = Q_2(p) - Q_1(p) = \beta_2\left[\ln\left(\frac{1}{1-p}\right)\right]^{1/\alpha_2} - \beta_1\left[\ln\left(\frac{1}{1-p}\right)\right]^{1/\alpha_1} \tag{2}$$

This expression is simple and depends on only four parameters: $(\alpha_1, \beta_1, \alpha_2, \beta_2)$, or equivalently $(\alpha_1, \beta_1, \Delta\alpha, \Delta\beta)$.

We observed (not shown here) that a change in the scale parameter β, keeping α fixed, gives the category "all precipitation quantiles intensify" for $\Delta\beta > 0$ and "all precipitation quantiles decrease" for $\Delta\beta < 0$. In opposition, a change in the shape parameter α while keeping β fixed gives either a U-shape for $\Delta\alpha < 0$ and a reversed U-shape

category for $\Delta\alpha > 0$. Note that when β is fixed, then the percentile of inversion is also fixed, at a precise rank, $p_{inv} = 1 - e^{-1} \approx 63\%$.

When both parameters change at the same time, their two effects will add up, with a weight depending on the relative change of α and β. Considering small relative changes, that is, $\frac{\Delta\alpha}{\alpha} \ll 1$ and $\frac{\Delta\beta}{\beta} \ll 1$, the quantile trends for a Weibull law can be written, at the first order, as:

$$\forall p \in (0,1),\ \Delta Q(p) \approx \frac{\partial Q}{\partial \alpha}(p)\ \Delta\alpha + \frac{\partial Q}{\partial \beta}(p)\ \Delta\beta \tag{3}$$

with the following expressions for the partial derivatives:

$$\frac{\partial Q}{\partial \alpha}(p) = -\frac{\beta}{\alpha^2}\ln\left(\ln\frac{1}{1-p}\right)\left(\ln\frac{1}{1-p}\right)^{1/\alpha}$$
$$\frac{\partial Q}{\partial \beta}(p) = \left(\ln\frac{1}{1-p}\right)^{1/\alpha}$$

The sensitivity of the trend curve to the two parameters α and β can be expressed as a simple ratio:

$$\left|\frac{\frac{\partial Q}{\partial \alpha}(p)\Delta\alpha}{\frac{\partial Q}{\partial \beta}(p)\Delta\beta}\right| = \frac{\beta}{\alpha^2}\left|\frac{\Delta\alpha}{\Delta\beta}\right|\left|\ln\left(\ln\frac{1}{1-p}\right)\right| \tag{4}$$

The change in α dominates the trend curve if it dominates the trends of at least the low percentiles and the tail. When plotting the logarithmic function $p \to \left|\ln\left(\ln\frac{1}{1-p}\right)\right|$ on $p \in [0, 1]$, we can show that this term is of order unity (except in the very near vicinity of the extremes percentiles 0 and 1 and of the inversion percentile $p = 1 - e^{-1}$). Thus, we will take the approximation that the logarithmic term is of order unity on the ranks that are of interest for distinguishing between the four different regimes. Finally, we come to the following result: the change in α dominates over β in the quantile trend curve when:

$$\left|\frac{\Delta\alpha}{\alpha^2}\right| \gg \left|\frac{\Delta\beta}{\beta}\right| \tag{5}$$

This means that knowing which of the changes of α or β dominates the trend curve boils down to comparing their normalized changes.

Therefore, in the space $\left(\frac{\Delta\beta}{\beta}, \frac{\Delta\alpha}{\alpha^2}\right)$, the two diagonals $\left(\left|\frac{\Delta\beta}{\beta}\right| = \left|\frac{\Delta\alpha}{\alpha^2}\right|\right)$ theoretically set the approximate limits between the four precipitation quantile trend regimes. More precisely, we expect.

- a U-shape for $\left|\frac{\Delta\beta}{\beta}\right| \ll \left|\frac{\Delta\alpha}{\alpha^2}\right|$ and $\Delta\alpha < 0$
- a reversed U-shape for $\left|\frac{\Delta\beta}{\beta}\right| \ll \left|\frac{\Delta\alpha}{\alpha^2}\right|$ and $\Delta\alpha > 0$
- all quantiles intensify for $\left|\frac{\Delta\beta}{\beta}\right| \gg \left|\frac{\Delta\alpha}{\alpha^2}\right|$ and $\Delta\beta > 0$
- all quantiles decrease for $\left|\frac{\Delta\beta}{\beta}\right| \gg \left|\frac{\Delta\alpha}{\alpha^2}\right|$ and $\Delta\beta < 0$

Therefore, the 2-parameters Weibull model seems a pertinent representation of the four regimes.

We can validate this theoretical result on ERA5 precipitation data by comparing the theoretical limits from the Weibull model between the four regimes with the classification obtained by the detection algorithm (which doesn't make any assumption about a distribution model). In Figure 1c, we plotted all grid-points of the domain in the normalized Weibull phase space, and colored them by their category as detected by the classification algorithm. The bottom quadrant of the plot is mainly occupied by "U-shape" gridpoints (orange), the left quadrant mainly "all decrease" category (red) and the right one mainly "all quantiles intensify" (green) points.

Note that the inference uncertainties on α and β parameters have little influence on these results. Indeed, the only locations which regimes deduced from Weibull parameters can be impacted by the fit errors are those near the diagonals and the center of the Weibull phase plot, that is, points which lie at the limits between two categories (see Appendix C). Furthermore, these points are at the same geographical locations where both $\Delta\alpha$ and $\Delta\beta$ are small and not significant, therefore where the wet-days regimes are considered as not robust.

Thus, the Weibull analytical limits from the diagonals are in very good agreement with the empirical categories.

Additionally, we can obtain an expression of the wet-days inversion percentile rank, p_{inv}, from the changes of α and β (see Appendix F for more details):

$$p_{inv} \approx 1 - \exp\left(-\exp\left(\frac{\Delta\beta}{\beta}\frac{\alpha^2}{\Delta\alpha}\right)\right). \tag{6}$$

which can be read graphically in the phase space $\left(\frac{\Delta\beta}{\beta}, \frac{\Delta\alpha}{\alpha^2}\right)$, from the angle a point makes with the horizontal.

4.3. Consequences for the Wet-Days Categories

Since the Weibull distribution enables a description of the four regimes by the relative change of the models' two parameters α and β, we can obtain information on the significance of the regimes from α and β. We assimilate the robustness of the wet-days categories to the statistical significance of Weibull parameters change: a "all quantiles intensify" and "all quantiles decrease" regimes are considered as robust if $\Delta\beta$ is statistically significant. Similarly, the "U-shape" and "reverse U-shape" regimes are considered as robust if $\Delta\alpha$ is statistically significant.

The results of the significant test are shown in Figure 5 (more details about the test in Appendix E). It shows that the Mediterranean region doesn't have a significant signal on wet-days categories, while in most parts of northern Europe, the "All quantiles intensify" regime is statistically significant. This result is consistent with our intuition we had, which was based on the stronger dependence of the Mediterranean regimes with the definition of the two time periods.

In summary of this section, we have used a Weibull model on the wet-days precipitation distribution to reduce the information of the quantile trend curve to only two parameters (α, β) and their changes ($\Delta\alpha$, $\Delta\beta$). These parameters are enough to separate between the four observed wet-days regimes, and the statistical significance of $\Delta\alpha$ and $\Delta\beta$ indicates the robustness of the wet-days regimes.

5. Influence of the Changes of Both the Wet-Days Distribution and Dry-Days Frequency

5.1. Impact on Annual Mean

In order to illustrate the importance of taking into account not only the wet-days distribution but also the change of the dry-days frequency, we study their relative contributions to the all-days mean precipitation (i.e., total annual precipitation), which is one of the most studied parameters in climate change studies.

The all-days mean $\bar{x}$ is the mean of the daily precipitation intensity, and can be equivalently computed as the product of the wet-days frequency $f_w = 1 - f_d$ with the wet-days precipitation mean μ:

$$\bar{x} = \left(1 - f_d\right)\mu$$

The change of the all-days mean is due both to the change of dry-days frequency $f_d = 1 - f_w$ and to the change of wet-days mean:

$$\frac{\Delta\bar{x}}{\bar{x}} = -\frac{\Delta f_d}{\left(1 - f_d\right)} + \frac{\Delta\mu}{\mu} \tag{7}$$

Those two terms can either be of the same sign and add up to each other, or be of opposite signs and tend to cancel each other out. Indeed, there could be more wet-days but with less intense precipitation, which could result in an

almost zero trend on the mean precipitation. Conversely, there could be regions with fewer wet-days but with higher precipitation intensity, as was shown in future projections by Pierce et al. (2013) for California and by Polade et al. (2014) for Mediterranean type climates. The relative weight of the two terms is also important to study. For future projections, Polade et al. (2014) showed that the change in the occurrence term will dominate the change in intensity for the all-days mean, in most of the subtropics. However, there is very little literature on the behavior of these two terms in past data.

For a Weibull distribution, we can further detail the dependency of the wet-days mean on the shape and scale parameters. The expression of the Weibull mean is $\mu = \beta\,\Gamma(1 + 1/\alpha)$, where Γ denotes the Gamma function. Taking the logarithmic derivative of the mean, and using the definition of the Digamma function (usually noted ψ) as the derivative of the log of the Gamma function, we get:

$$\frac{\Delta\mu}{\mu} \approx \frac{\Delta\beta}{\beta} - \frac{\Delta\alpha}{\alpha^2}\left(\frac{d\,\ln\Gamma}{dz}\right)_{z=1+1/\alpha} = \frac{\Delta\beta}{\beta} - \frac{\Delta\alpha}{\alpha^2}\psi(1 + 1/\alpha) \tag{8}$$

Note that the Digamma function is strictly positive for the typical range of the shape parameter for ERA5 precipitation, thus the sign of the shape parameter contribution is given by $-\Delta\alpha$. Its typical values are $\psi(1 + 1/\alpha) \in [0.4, 1]$, for $\alpha \in [0.5, 1]$, which is the typical range for Europe and the Mediterranean. Thus, even in regions with a U-shape categories, where $\Delta\alpha$ dominates the wet-days trend curve as $\frac{|\Delta\beta|}{\beta} < \frac{|\Delta\alpha|}{\alpha^2}$, the change in wet-days mean is not necessarily dominated by $\Delta\alpha$, since the Digamma factor is smaller than 1.

Note that the Weibull model captures most of the signal of the relative change of mean precipitation, with an error of less than 1% on most parts of the domain, aside from desert (see Appendix D for more details).

Finally, the relative change of the all-days mean can be decomposed in three contributions, from the relative changes of f_d, α and β:

$$\frac{\Delta\bar{x}}{\bar{x}} \approx -\frac{\Delta f_d}{(1 - f_d)} + \frac{\Delta\beta}{\beta} - \frac{\Delta\alpha}{\alpha^2}\,\psi(1 + 1/\alpha) \tag{9}$$

Figure 2 shows the relative contributions of those terms to the all-days mean change, and the significance of these changes. We have a clear North–South pattern for the change of total precipitation and of dry-days occurrence.

For northern Europe, the contributions of occurrence and intensity changes are of same sign (decrease of dry-days frequency and more intense precipitation in average), but the all-days mean change is mainly due to the increase of the wet-days mean (the latter being mainly due to the increase of the Weibull scale parameter β). We see also that the intensity change is significant over a larger region than the occurrence change, in Northern Europe.

For the Mediterranean region, on the contrary, the intensity change is mainly not significant, while the increase of dry-days frequency is homogeneous and significant, leading to a significant decrease of all-days mean. In a central European band between East France and Poland, the change of occurrence is close to zero, and the change in wet-days intensity is the sole contributor to the all-days mean.

Both in northern Europe and in the Mediterranean (even in U-shape regions), the changes of the wet-days mean are mainly due to the significant change of the scale parameter β, while the term due to the change of the scale parameter α is smaller in intensity and not significant.

5.2. Influence on All-Days Quantiles Trends of the Dry-Days Frequency

In this section, we investigate in more detail the link between all- and wet-days precipitation quantiles. In order to understand and quantify how looking only at wet-days can impact the values of the trends for all-days quantiles, we follow the framework proposed by Schär et al. (2016), more precisely the derivation made in their first appendix.

The all-days precipitation distribution is linked to the wet-days' one by the dry-days frequency f_d. More precisely, the wet-days percentile p, which denotes the probability of having an event of intensity smaller or equal than x mm/day, and the all-days percentile p_a for the same precipitation intensity, are linearly linked by f_d:

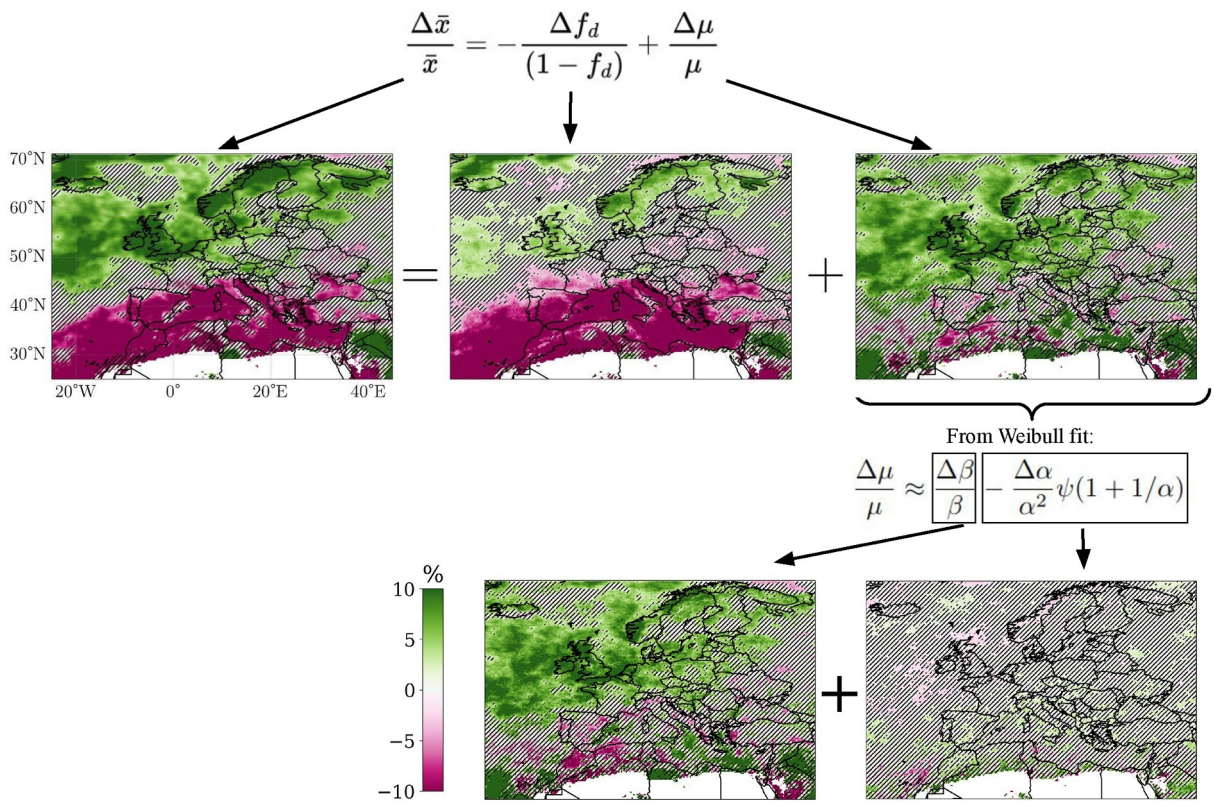

Figure 2. The relative change between 1950–1980 and 1990–2020 of the all-days precipitation mean $\bar{x}$, decomposed in its different contributions, from the changes of dry days frequency f_d and the wet-days mean μ, the latter further decomposed into contributions from Weibull two parameters, α and β. Every map has the same scale for the color-map. The hatches show the zones where the changes are not significant, with bootstrap test at 90% confidence level.

$$p_a = (1 - f_d)p + f_d \tag{10}$$

Note that this formula is valid for any percentile rank as far as $p_a \geq f_d$. It gives indeed that for $p = 0$ we have $p_a = f_d$ and that the probability of the maximum precipitation value is the same ($p = 1$ when $p_a = 1$). This simple formula shows that a wet-days percentile p is linearly linked to the all-days percentiles p_a.

By definition, the wet-days quantile Q is equal to the all-days quantile Q_a for percentiles where they are both defined:

$$\forall p_a \in [f_d, 1], Q(p) = Q_a(p_a) \tag{11}$$

We now consider a change between the two time periods, 1 and 2, of the wet-days precipitation distribution and its quantiles Q: $\Delta Q = Q_2 - Q_1$, where Δ denotes again the change. For a fixed wet-days percentile p, ΔQ is related to the change of the all-days rank and quantile intensity, but also to the change in dry-days frequency. Rewriting with our notations the Equation A7 from the appendix of Schär et al. (2016) gives:

$$\Delta Q(p) = \Delta Q_a(p_a) + \frac{\Delta f_d}{1 - f_d}(1 - p_a)\frac{\partial Q_{a,2}}{\partial p_a} \tag{12}$$

We would like to express analytically the slope of the quantile curve $\frac{\partial Q_{a,2}}{\partial p}$, with the Weibull model developed earlier. Thus, we come back to the slope of the wet-days quantiles, by using Equation 11 and the chain rule:

$$\frac{\partial Q_{a,2}(p_a)}{\partial p_a} = \frac{\partial Q_2(p)}{\partial p_a} = \frac{\partial Q_2(p)}{\partial p}\frac{\partial p}{\partial p_a}$$

Since the percentiles p and p_a are linearly linked, $\frac{\partial p}{\partial p_a} = \frac{1}{1-f_d} = \frac{1-p}{1-p_a}$, we get the following relationship between the two quantiles slopes:

$$(1-p_a)\frac{\partial Q_{a,2}}{\partial p_a} = (1-p)\frac{\partial Q_2}{\partial p}$$

Thus, Equation 12 becomes:

$$\Delta Q(p) = \Delta Q_a(p_a) + \frac{\Delta f_d}{1-f_d}(1-p)\frac{\partial Q_2}{\partial p} \tag{13}$$

Finally, we can apply the general formula in Equation 13 to a Weibull distribution of shape parameter α and scale parameter β. Putting all the terms depending on the wet-days percentile p on the same side, it yields:

$$\Delta Q_a(p_a) = \Delta Q(p) - \frac{\Delta f_d}{(1-f_d)}\underbrace{\frac{\beta_2}{\alpha_2}\left[\ln\left(\frac{1}{1-p}\right)\right]^{1/\alpha_2-1}}_{\text{distorting term}} \tag{14}$$

This equation shows that the quantile trends in all-days can differ from the wet-days trends due to the change of precipitation occurrence, which acts as a weight in front of a distorting term (underlined by a curly brace in equation Equation 14). Note that the distorting term is growing with p and its form changes with the shape parameter α, giving even larger additive trends for the heavy precipitation percentiles as α is small. Note that in the limit case where $\alpha \to 1$, this distorting term becomes a shift of constant value β_2: it is not anymore distorting the wet-days trend curve.

5.3. Modified Regimes for All-Days Quantile Trends

On historical data, it is important to quantify when and where the change of occurrence is large enough, compared to the wet-days quantile trends, to create relevant changes on the all-days quantile curves. We also want to analyze which percentiles' all-days trends will be the most impacted by Δf_d. We thus need to compare the Δf_d term to the $\Delta Q(p)$ term, in Equation 13.

The all-days trend is given by the wet-days trend if and only if, $\Delta Q_a(p_a) \approx \Delta Q(p)$ that is, $|\Delta Q(p)| \gg \left|\frac{\Delta f_d}{1-f_d}\frac{\beta_2}{\alpha_2}\left[\ln\left(\frac{1}{1-p}\right)\right]^{1/\alpha_2-1}\right|$. At the first order, it is true if and only if:

$$\left|\frac{\partial Q}{\partial \alpha}(p)\Delta\alpha + \frac{\partial Q}{\partial \beta}(p)\Delta\beta\right| \gg \left|\frac{\Delta f_d}{1-f_d}\frac{\beta}{\alpha}\left[\ln\left(\frac{1}{1-p}\right)\right]^{1/\alpha-1}\right|$$

where we noted $\alpha = (\alpha_1+\alpha_2)/2 \approx \alpha_2$ and similarly for β. Let's look whether at least one of the two left-hand side terms is dominant over the term in Δf_d. The term due to the change of the scale parameter of the wet-days distribution, $\left|\frac{\partial Q}{\partial \beta}(p)\Delta\beta\right|$, dominates over the change of occurrence term for percentiles p such as:

$$\left|\ln\left(\frac{1}{1-p}\right)\right| \gg \left|\frac{\Delta f_d}{1-f_d}\frac{\beta}{\Delta\beta}\frac{1}{\alpha}\right|. \tag{15}$$

This is verified at least for rank a rank $p < 1$ since $\lim_{p\to 1}\ln\left(\frac{1}{1-p}\right) = +\infty$. This independence of the maximum precipitation event trend from the precipitation occurrence was to be expected from Equation 10: $p = 1$ and $p_a = 1$ both describe the same event in wet-days and all-days. In addition, since the function $p \to \ln\left(\frac{1}{1-p}\right)$ is strictly

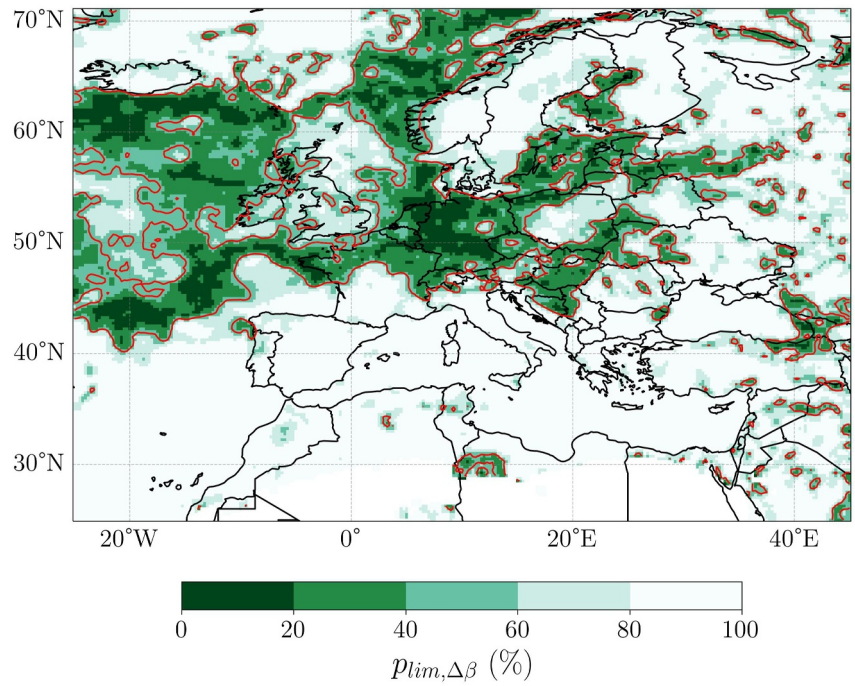

Figure 3. Limit percentiles $p_{\lim,\Delta\beta}$ after which the impact of the precipitation occurrence trend can be neglected for a wet-days quantile trends, thanks to the large trend of Weibull parameter β. The thin red contour denotes the value of 50%.

growing on [0,1] up to infinity, there exists a percentile $p_{\lim,\Delta\beta}$ above which the function becomes larger than $|\frac{\Delta f_d}{1-f_d}\frac{\beta}{\Delta\beta}\frac{1}{\alpha}|$.

$$\exists p_{\lim,\Delta\beta} \in [0,1], \left|\ln\left(\frac{1}{1-p_{\lim,\Delta\beta}}\right)\right| = \left|\frac{\Delta f_d}{1-f_d}\frac{\beta}{\Delta\beta}\frac{1}{\alpha}\right|. \tag{16}$$

Thus, quantiles of ranks between $p_{\lim,\Delta\beta}$ and $p = 1$ (the maximum precipitation event) can be considered as not impacted by the change of dry-days.

As for the term due to the change of the shape of the wet-days distribution, it is only dominant over the change of occurrence term for percentiles p such as:

$$\left|\ln\left(\frac{1}{1-p}\right)\ln\left(\ln\frac{1}{1-p}\right)\right| \gg \left|\frac{\Delta f_d}{1-f_d}\frac{\alpha}{\Delta\alpha}\right|. \tag{17}$$

The left-hand side function is strictly growing on $[1-e^{-1}, 1]$ and tends to infinity at 1, thus there also exists a percentile rank $p_{\lim,\Delta\alpha}$ above which this term becomes larger than $|\frac{\Delta f_d}{1-f_d}\frac{\alpha}{\Delta\alpha}|$.

These two limit percentiles, which we will call $p_{\lim,\Delta\alpha}$ and $p_{\lim,\Delta\beta}$, can be inverted either analytically or numerically (e.g., using the segment or tangent methods).

On ERA5 precipitation data, the resulting percentile $p_{\lim,\Delta\alpha}$ is very high in both Europe and the Mediterranean (mostly above 95%, not shown) which means that the term in $\Delta\alpha$ is almost never dominant compared to the one in Δf_d for the all-days trend $\Delta Q_a(p_a)$.

On the other hand, the limit percentile $p_{\lim,\Delta\beta}$ can reach lower values and has more spatial variability (see Figure 3). For the Mediterranean, $p_{\lim,\Delta\beta}$ is very large (close to 100%). Thus, for the great majority of percentile ranks in the Mediterranean, the all-days trends are mainly due to the decrease of dry-days frequency and not to a change of intensity when it rains. This is consistent with the low statistical significance of $\Delta\alpha$ and $\Delta\beta$ over the Mediterranean on ERA5 data, while Δf_d is strong and significant.

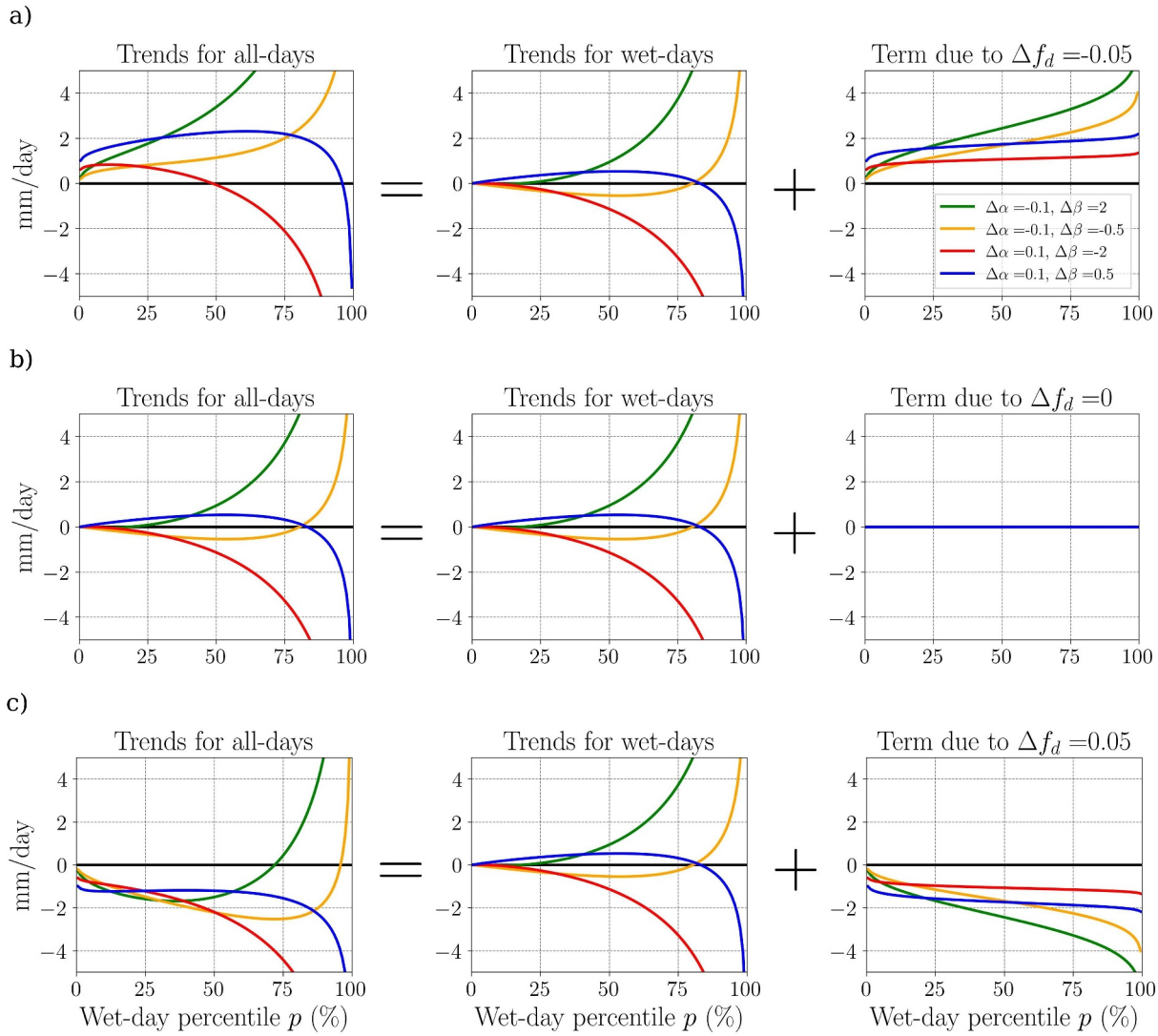

Figure 4. Illustration of the influence of the dry-days frequency term on the all-days quantile trend curves, for the four categories, for different values of the dry-days frequency change Δf_d: $\Delta f_d = -5\%$ (a), $\Delta f_d = 0\%$ (b), $\Delta f_d = 5\%$ (c). The values of the wet-days Weibull parameters (α, β, $\Delta\alpha$ and $\Delta\beta$) are the same for all the subplots and are given on the top row, and are synthetic.

For most of central and north Europe (aside of the Scandinavia), $p_{\mathrm{lim},\Delta\beta}$ reaches much lower values: it is below 50% on about half of these regions' surface, and can go as low as 10%. Thus, in these regions, the influence of the change of dry-days frequency can be neglected compared to the change of the wet-days scale parameter, for wet-days percentiles larger than $p_{\mathrm{lim},\Delta\beta} \approx 50\%$.

Let us now study the all-days trend curves, and how the all-days categories can differ from the wet-days' in the case of a strong change of occurrence. Figure 4 displays three typical cases, depending on the sign of the occurrence change.

It shows that in regions where the precipitation occurrence increases strongly enough, some locations with U-shape wet-days regime can become "all-increase" all-days regime (provided that the Δfd term is large enough), while the wet-days "all-increase" trends can be even stronger. Similarly, wet-days "all-decrease" will merge with "reversed U-shape" to give a new all-days "reversed U-shape." Thus, only two main regimes could exist for such regions in all-days distribution: "all-increase" and "reversed U-shape."

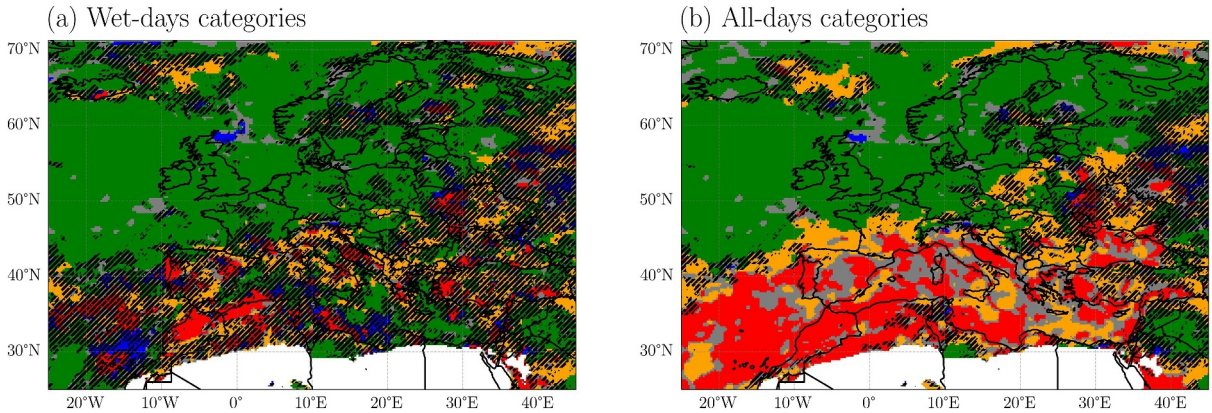

Figure 5. Category maps for the 1950–1980 and 1990–2020 periods. As before, green corresponds to "all quantiles intensify" category, red to "all quantiles decrease", orange to "U-shape" and blue to "reversed U-shape", while points whose category was unclear are in gray. White designates desert location (less than 2% of wet-days). The hatches on the left figure (resp. right figure) denote the location where neither $\Delta\alpha$ nor $\Delta\beta$ (resp. neither $\Delta\alpha$ nor $\Delta\beta$ nor Δf_d) are significant through a bootstrap test, at a confidence level of 90%.

In regions where the precipitation occurrence decreases strongly (like in the Mediterranean), the opposite occurs: the "all-increase" wet-days regime will disappear in favor of an all-days "U-shape" regime, while wet-days U-shape's inversion percentile will become even larger in all-days. Similarly, the "reversed U-shape" will merge with the "all-decrease" category. Thus, only two all-days regimes would be expected in regions with a strong decrease of f_d: "U-shape" and "all-decrease."

Therefore, we expect that the Mediterranean all-days quantile trend curves will be mainly due to the increase of dry-days frequency, leading to a "all-decrease" category, different from the wet-days non-significant categories.

In opposition, for most of northern Europe, all-days quantile trend curves are expected to be very similar to the wet-days', as the influence of $\Delta\beta$ is dominant over the change of dry-days there.

We can check this theoretical conclusion again on the all-days categories maps. We can naturally define an extension of the detection algorithm from wet-days quantile curves (as presented in Section 3) to all-days quantiles curves. It consists in computing the all-days quantile trends (from percentiles $p_a \in [0, 1]$) and then applying the algorithm only the right part of the curve: only on the equivalent wet-days percentiles p_w corresponding to $p_a \in [f_d, 1]$, with f_d the dry-days frequency of the reference period (1950–1980). This all-days detection algorithm enables to focus on the rainy quantiles, nevertheless incorporating the change of dry-days frequency.

Figure 5 shows the results for the all-days category map, and the already shown wet-days category map. The maps are put side by side to better highlight the differences due to the change of dry-days frequency, which are as we predicted above. In terms of spatial pattern, the overall North–South pattern of all-days category map is even clearer than the wet-days', and the map is overall smoother. In all-days categories, there is a continuous transition in latitude, from "all increase" in the North to "all decrease" in the South, and "U-shape" or "Mediterranean paradox" transition zone in between. Thus, the Mediterranean paradox is found in this transitional zone between the wetting in northern Europe (due to the increase of both precipitation intensity and occurrence) and the strong drying in the Mediterranean (due to the decrease of occurrence).

The significance of the wet-days categories is associated to the one of the Weibull scale parameter change $\Delta\beta$, while we consider all-days categories as significant when either $\Delta\beta$ or Δf_d are significant. The significance results in Figure 5 highlight the fact that the signal of precipitation change in the Mediterranean in the last 70 years is not due to the change in wet-days distribution, but to the decrease of the dry-days frequency (which impacts the whole all-days distribution).

6. Conclusion

Climate change is known to impact greatly the Mediterranean region, which overall becomes warmer and drier, while the effects on extreme precipitation is still quite debated on historical data (Ali et al., 2022). In this study we aimed at better understanding how the strong trends of drying of the Mediterranean can influence the distribution of precipitation, all-together with the change of the whole wet-days distribution itself (from the low and medium percentiles to the most extreme precipitation).

Using the ERA5 reanalysis, we studied the evolution of the wet-days precipitation distribution in the recent past, since the 1950s. We showed that it could evolve in four different regimes, defined on the quantiles trends curves: "all precipitation quantiles intensify," "all precipitation quantiles decrease," "U-shape" and "reversed U-shape." The map of the four regimes computed over Europe and the Mediterranean shows a strong contrast between these two regions. While in northern Europe all quantiles are intensifying with a clear and robust signal, the Mediterranean's regimes are shared between a dominant "U-shape" regime mixed with "all quantiles decrease," but are overall more spotty due to strong natural variability. This suggests that a climate change signal and its impact on the wet-days precipitation distribution, shift or distortion, have not (or not yet) emerged in the Mediterranean region, contrary to northern Europe.

As for the map of regimes for the all-days distribution, it shows a clearer signal with latitude, from the Mediterranean ("all decrease") with a smooth transition (through a "U-shape" regime) to northern Europe ("all increase" regime). The greater spatial uniformity of the all-day regime map in the Mediterranean comes from the stronger and more robust signal of dry-days frequency change, which dominates the all-day distribution trends.

By modeling the wet-days distribution with a Weibull law, we were able to reduce the information of the quantile trends to just two parameters, a scale and shape parameters, and their changes (representative of the precipitation distribution shift and distortion respectively). The categorization in four regimes can be estimated directly from the ratio and signs of the relative changes of the two Weibull parameters, as can be done for the percentile of inversion, when it exists. A statistical significance test on the change of the Weibull parameters confirms that a signal has emerged in Europe, with a strong increase of the scale parameter, that is, a shift of the whole distribution to more intense precipitation, without distortion. In the Mediterranean, only a few small regions have significant change of scale or shape parameter, reinforcing the argument that a climate change signal on wet-days has not yet emerged from natural variability.

Coming back to the whole distribution (including dry-days), we quantified how much some all-days important variables, such as the trends of the annual mean or of quantiles, are influenced by both the change of wet-days distribution and of dry-days frequency (the latter significantly increases in the Mediterranean but decreases in northern Europe). The two effects can add up (as for the all-days mean in most of northern Europe) or counterbalance each other (as in southern Italy or in Poland).

The resulting all-days category map shows a clearer signal in latitude than the wet-days one: there is mostly "all precipitation quantiles intensify" in northern Europe, then a transition with "U-shape" in a thin band of central Europe, and finally the"all precipitation quantiles decrease" regime in most of the Mediterranean. Note that the so called Mediterranean paradox, that is, "U-shape" regime in all-days, is thus not present in most of Mediterranean region, while it was dominant over this region when only wet-days were considered.

One of the key findings of the paper is that the change of dry-days frequency is predominant for the all-days trends of most quantiles in the Mediterranean, while in northern Europe its effect can be neglected compared to the strong increase of the Weibull scale parameter, for all quantiles with wet-days rank above about 50%.

In a nutshell, the framework developed in this study establishes a connection between changes in wet-days precipitation and a few critical parameters that capture the shift and distortion of the precipitation distribution, as well as changes in precipitation occurrence. It has the potential to be employed in different geographical regions and time spans. In an upcoming publication, we intend to apply this framework to the future climate projections for the 21st century, in order to have a stronger and more robust signal over the Mediterranean. It would also enable to detect the year of emergence of the signal. Another potential application of this framework is the study of the physical processes that cause the observed changes, both from large-scale and local effects.

Appendix A: Influence of the Time Period

In Figure A1, we can see the wet-days category maps computed for different time periods, covering the 1950–2020 periods.

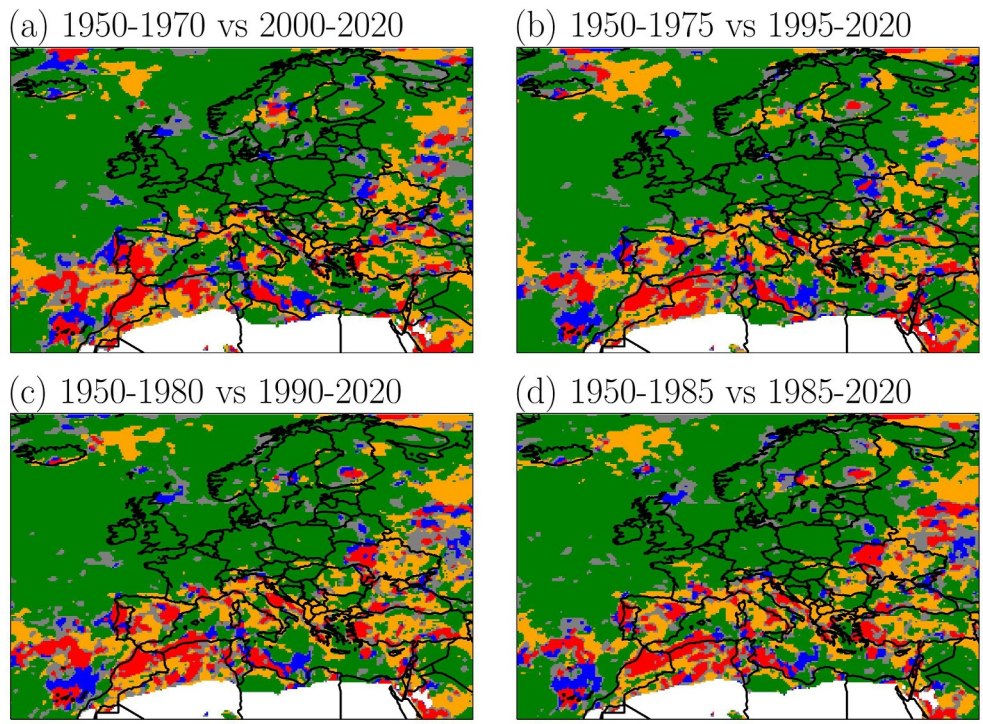

Figure A1. Category maps for wet-days quantile trends computed for different couples of time periods over 1950–2020. The quantile trends values leading to this map have been processed by a smoothing window of nine points. As before, green color corresponds to "all quantiles intensify" category, red to "all quantiles decrease", orange to "U-shape" and blue to "reversed U-shape."

- 1950–1970 versus 2000–2020
- 1950–1975 versus 1995–2020
- 1950–1980 versus 1990–2020
- 1950–1985 versus 1985–2020

At a given location, the category of the reference period is considered as robust if at least three of the four pairs of periods give the same category. This criterion is used to define both for wet-days and all-days category's robustness, which is represented by the gray hatches on Figure A2.

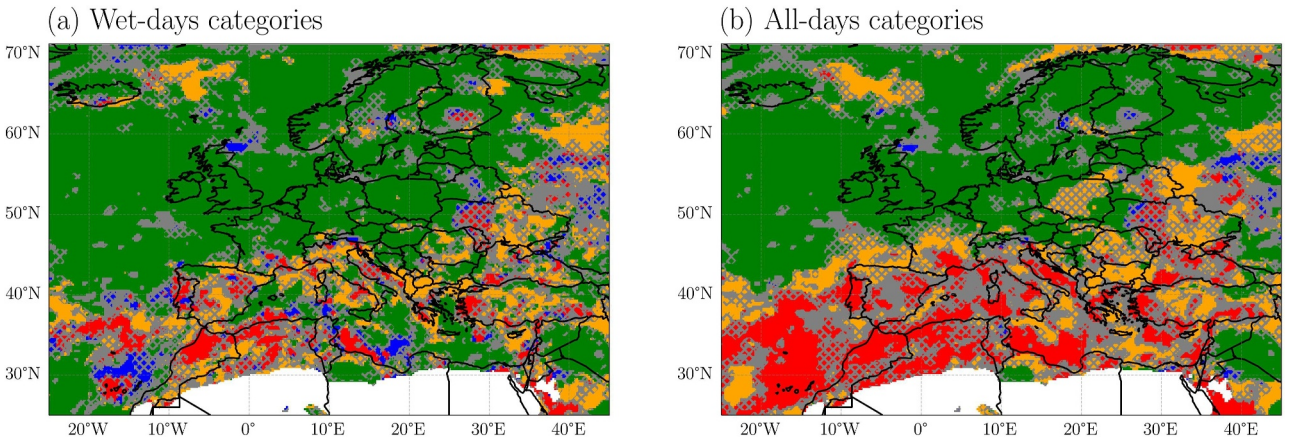

Figure A2. Category maps for the 1950–1980 and 1990–2020 periods. As before, green corresponds to "all quantiles intensify" category, red to "all quantiles decrease", orange to "U-shape" and blue to "reversed U-shape", while points whose category was unclear are in gray. White designates desert location (less than 2% of wet-days). The gray hatches denote places where the category detection is not very robust with regard to changes in the periods considered (cf. Appendix A).

On Figure A2 we see that both the wet-days and all-days category map are very robust with the time periods, over the northern part of Europe. However, in the Mediterranean, most places' categories are not as robust, especially when at the frontier between different categories. Overall, the North–South pattern of all-days and wet-days categories is robust to the time periods considered.

Appendix B: Comparison of Distribution Models for ERA5 Precipitation

There is no a priory clear choice for a parametric model for the whole wet-days distribution of daily precipitation (above threshold, here 1 mm/day). The choice of a particular model may depend a lot on the region considered, on the origin of the data (station data, spatial interpolation from stations, satellite data, reanalysis, or climate projections), on its spatial and temporal resolution, etc. We have therefore tested on ERA5 daily precipitation data, a list of the most common models (as well as the distribution from (Naveau et al., 2016), called Naveau in the following). To compare the quality of the different models, we used two goodness-of-fit estimators, computed on cumulative distribution functions: Kolmogorov-Smirnov (a L1 distance) and Cramer von Mises (a L2 distance). When a location parameter was needed, we set it at the wet-days threshold (1 mm/day).

The inference is done on the period 1950–1980, pulling all wet-days of a given location together, irrespective of their seasonal occurrence. We do not make the assumption of equal distribution of wet-days precipitation across season; we simply disregard the potential seasonal variation of the parameters.

We found that in average, the best distribution for the Mediterranean region was the Naveau law, followed by the Weibull law and the Gamma law (Figure B1). As the Naveau model has more complexity (three parameters) than

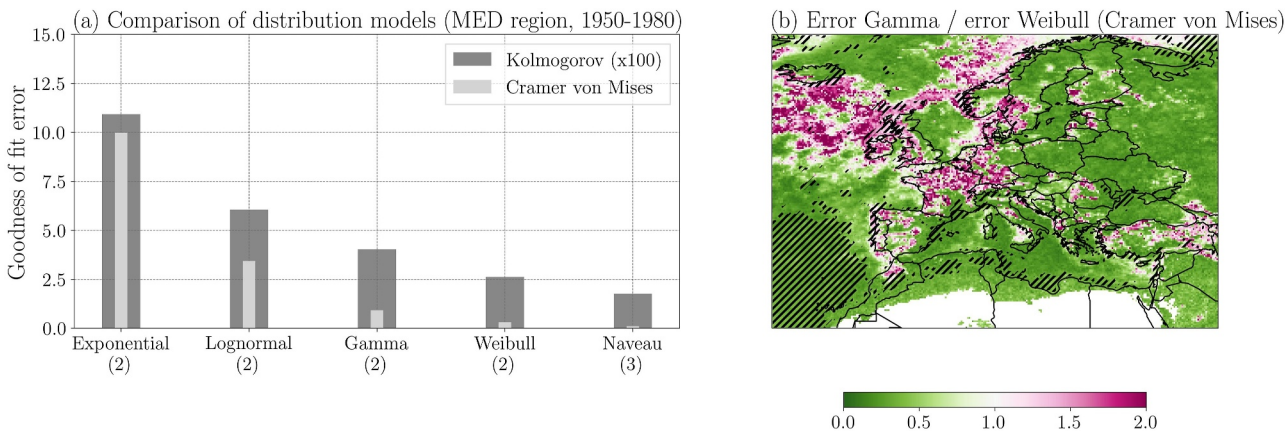

Figure B1. (a) Goodness-of-fit estimator for different wet-days distribution models in the Mediterranean region (as defined by the IPCC) on 1950–1980. Note that we used a scale factor for the Kolmogorov–Smirnov estimator, which was much smaller than Cramer von Mises estimator. In the *x*-axis, the number in parentheses is the number of parameters of the fit. (b) Map of the ratio of errors (here Cramer von Mises goodness-of-fit) between Gamma and Weibull models, across the whole domain, for the same period. In green are all the location where Weibull model is better suited for the data than Gamma. Black hatches show the locations where the adjustment test of the Weibull model fails, with a confidence level of 95%.

what we need to capture the quantile trends regimes, we decided not to select this model. We compared Weibull and Gamma laws pixel-wise across the whole Europe and Mediterranean. The ratio of the fitting error of Weibull versus Gamma laws shows that the Weibull model is more suitable than Gamma law, in most of the Mediterranean domain. We therefore choose the Weibull law for our model.

Once we fitted the Weibull law on a time serie and that we got its optimal fit parameters, we used the usual Kolmogorov-Smirnov distance as an adjustment test: if this distance is "small enough", the fit is accepted. According to empirical tables, for a confidence level of 95%, the Kolmogorov-Smirnov distance is considered small enough if falling below $1.36/\sqrt{N}$, where N is the number of data points, as far as $N > 35$ (which is largely the case since we fit Weibull on daily data on several decades). The mask of where the Weibull fit doesn't pass the adjustment test is shown by hatches on Figure B1. It shows that Weibull is indeed an acceptable model for most of the domain (except for some Mediterranean coastal areas and sea area in the Atlantic west of Portugal).

Appendix C: Weibull Parameters Values and Uncertainties

Figure C1 shows the values of the Weibull parameters for the wet-days distribution of ERA5 precipitation data, their trends and statistical significance (computed by a bootstrap test, as explained in Appendix E) and the uncertainties of the fit.

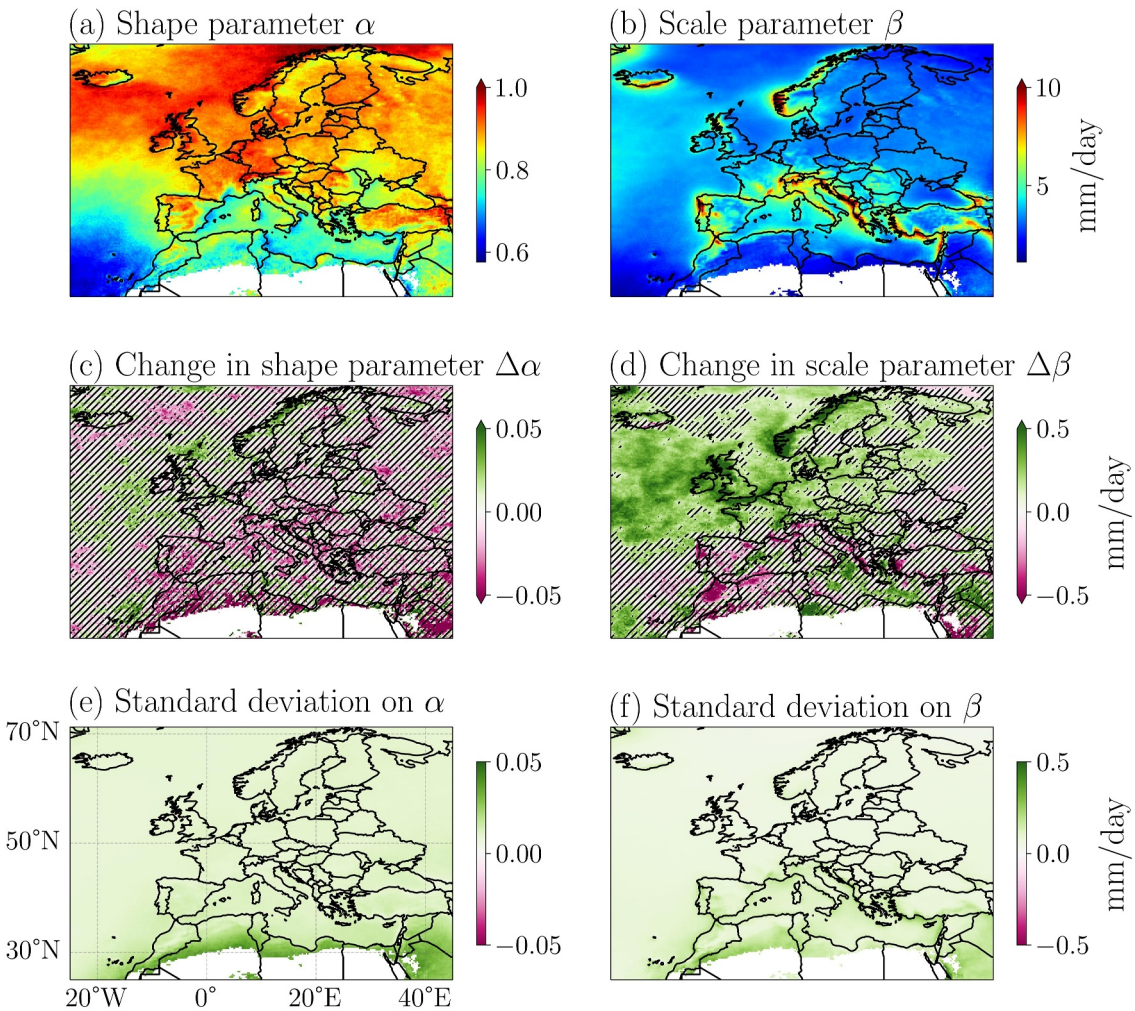

Figure C1. Results for the Weibull parameters fitted on ERA5 wet-days precipitation distribution. Top row: Weibull shape parameter α and scale parameter β on the period 1950–1980. Middle row: absolute changes between 1950–1980 and 1990–2020. The hatches denote the location where the change is not significant through a bootstrap test, at a confidence level of 90%. Bottom row: standard error of the Weibull parameters, on the period 1950–1980, estimated through the approximate normality of the log likelihood.

The uncertainties on the fit were quantified by the standard errors of each parameter, estimated through the approximate normality of the log-likelihood function, as presented in Coles et al. (2001), chapter 2.6. Though the values of a precipitation time serie are not independent and identically distributed, this method gives us an order of magnitude of the fit uncertainties. In practice, we used the Python package Reliability Reid (2022) to compute the standard error of each parameter.

We then checked if the standard errors on α and β parameters could change the category deduced by diagonal separation. More precisely, we looked at whether the four points around $\left(\frac{\Delta\beta}{\beta}, \frac{\Delta\alpha}{\alpha}\right)$ that is, $\left(\frac{\Delta\beta}{\beta}, \frac{\Delta\alpha \pm 2\sigma_\alpha}{\alpha}\right)$ and $\left(\frac{\Delta\beta \pm 2\sigma_\beta}{\beta}, \frac{\Delta\alpha}{\alpha}\right)$, lie in the same quadrant of the Weibull phase space. If the fit errors make the quadrant change, then we consider that the diagonal categorization is not robust to the inference uncertainty, for this location.

This happens for pixels which lie close to the diagonals and the center on the Weibull space, as shown in Figure C2. When this figure is compared to 5, it becomes clear that the places where the uncertainty on fit parameters interfere with the diagonal category detection are the places where neither $\Delta\alpha$ nor $\Delta\beta$ is significant, that is, the locations where the wet-days categories are considered are not significant. Therefore, the fit uncertainties do not impact the results presented in this article.

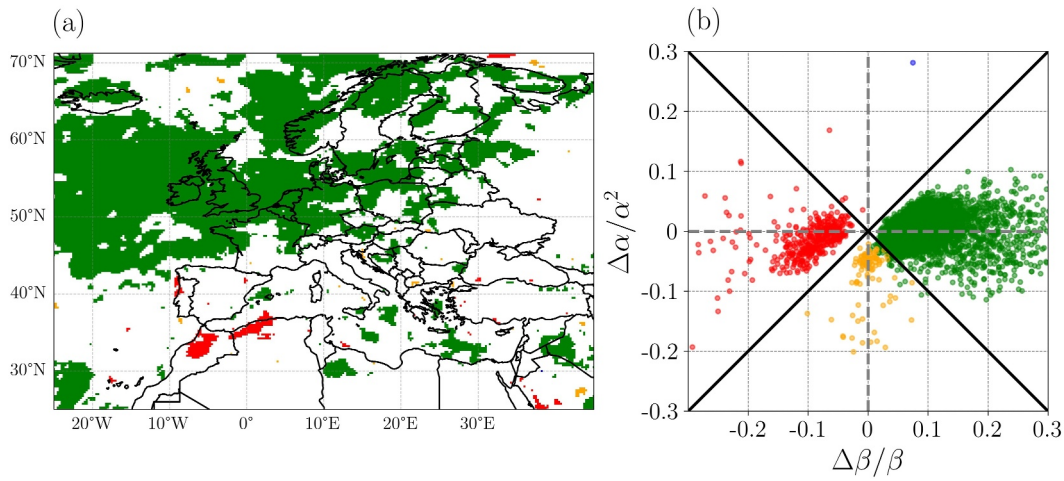

Figure C2. (a) Categories plotted for locations where diagonal separation method is robust with regard to the inference uncertainties. (b) These locations are plotted in the Weibull phase space.

Appendix D: Weibull Estimate of Mean Precipitation Trends

Here, we check how well the first order approximation of Equation 9 and Weibull model enable to capture the change in all-days means. We compare the all-days mean (computed directly from data) to the sum of the f_d, α and β terms in Equation 9, in Figure D1. This figure shows that the Weibull model for the intensity plus the precipitation occurrence capture most of the features of the all-days mean.

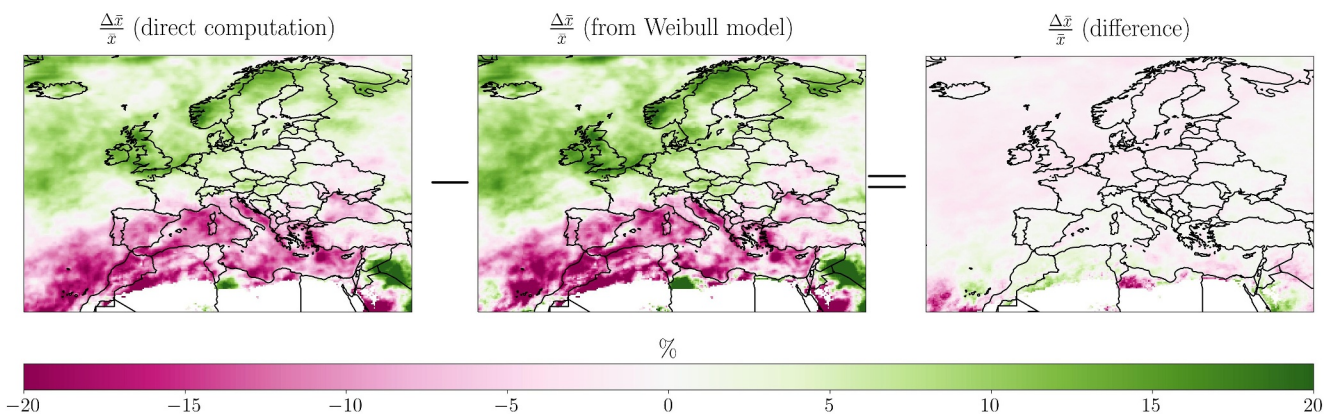

Figure D1. Relative change of all-days mean $\frac{\Delta\bar{x}}{\bar{x}}$, between 1950–1980 and 1990–2020, computed directly on data, compared to estimated from the Weibull model, that is, the three contributions from f_d, α and β.

Except for the lower latitudes where the error can reach 10%, the difference between the direct computation and the sum term is indeed only of a few percent, in Europe and the Mediterranean.

Appendix E: Statistical Significance Test

We are interested in their statistical significance of different statistics computed on the data, such as the quantile trends or the Weibull parameters trends. As the precipitation data in the Mediterranean region is spatially and temporally correlated, we perform a bootstrap test. It consists in comparing the trend of the real data with the trends that would be obtained on a large number (typically a hundred) of artificial samples presenting a spatial and temporal variability similar to our original data. Each sample is an artificial time serie created by pulling random days (and the corresponding precipitation map over the domain) from our 1950–2020 original data. The random pulling is done with replacement. The artificial time series created have the same length as the original one.

Since the dates have been mixed in the artificial samples, their average linear trends are zero, but their variability gives us an estimation of the noise in our original data. The trend of the original data is said significant at a given level, for example, 90%, if the original data lies within the 10% more extreme values of the bootstrap distribution, meaning that we could have the original data "by chance" from this random distribution only with low probability (less than 10%).

Appendix F: Inversion Percentile

When the regime is a "U-shape", the quantile curve has negative trends up to a certain percentile rank, which we will define as the "inversion percentile." After that rank, almost all the following percentiles have positive trends. We can get an analytical expression for the inversion percentile p_{inv} with the Weibull model, by solving the equations $\Delta Q(p_{inv}) = 0$ for $p_{inv} > 0$. This results in the following expression:

$$p_{inv} = 1 - \exp\left(-\left(\frac{\beta_2}{\beta_1}\right)^{\frac{\alpha_1\alpha_2}{\alpha_2-\alpha_1}}\right) \tag{F1}$$

Since the changes of α and β are small for precipitation in ERA5 data (about a few percents), we can simplify this expression. Let's write $\Delta\alpha = \alpha_2 - \alpha_1$ and $\alpha = (\alpha_2 + \alpha_1)/2$, and similarly for β, then we have $\frac{\beta_2}{\beta_1} \approx 1 + \frac{\Delta\beta}{\beta}$ and $\frac{\alpha_1\alpha_2}{\alpha_2-\alpha_1} \approx \frac{\alpha^2}{\Delta\alpha}$, and we can simplify the exponent:

$$\ln\left(\frac{\beta_2}{\beta_1}^{\frac{\alpha_1\alpha_2}{\alpha_2-\alpha_1}}\right) = \frac{\alpha_1\alpha_2}{\alpha_2-\alpha_1}\ln\left(\frac{\beta_2}{\beta_1}\right) \approx \frac{\alpha^2}{\Delta\alpha}\ln\left(1+\frac{\Delta\beta}{\beta}\right) \approx \frac{\alpha^2}{\Delta\alpha}\frac{\Delta\beta}{\beta}$$

where the last approximation is done by taking the development at the first order in $\Delta\beta/\beta$. We finally get this expression for the inversion percentile:

$$p_{inv} \approx 1 - \exp\left(-\exp\left(\frac{\Delta\beta}{\beta}\frac{\alpha^2}{\Delta\alpha}\right)\right) \tag{F2}$$

Geometrically speaking, this means that at first approximation, the angle in the Weibull parameter space $(X,Y) = \left(\frac{\Delta\beta}{\beta}, \frac{\Delta\alpha}{\alpha^2}\right)$ gives the value for the inversion percentile p_{inv}.

We can also derive a lower and upper limit for the inversion percentile. Indeed, the inversion percentile is properly defined only in the case where the change of α dominates (U-shape or reversed U-shape), that is, when $|\frac{\Delta\alpha}{\alpha^2}\frac{\beta}{\Delta\beta}| \gg 1$. The limit cases for this to be true would be when the change in α doesn't dominate anymore, that is, when $\frac{\Delta\alpha}{\alpha^2}\frac{\beta}{\Delta\beta}$ is close to -1 or 1. Those two cases give the minimal and maximal values of p_{inv} for a U-shape according to the Weibull law are: $p_{0,\min} \approx 1 - e^{-e^{-1}} \approx 30\%$ and $p_{0,\max} \approx 1 - e^{-e^{1}} \approx 93\%$. These values are consistent with the range of inversion percentile observed on the reanalysis (not shown).

Data Availability Statement

The hourly precipitation variable in ERA5 reanalysis Hersbach et al. (2018) was downloaded from the Copernicus Climate Change Service (C3S) accessed in July 2022. It is freely available on C3S website. The results contain modified Copernicus Climate Change Service information 2020. Neither the European Commission nor ECMWF is responsible for any use that may be made of the Copernicus information or data it contains.

Acknowledgments
CJM gratefully acknowledge funding from the European Research Council (ERC) under the European Union's Horizon 2020 research and innovation program (Project CLUSTER, Grant Agreement No 805041). The authors also thank Samuel Somot (Centre National de Recherches Météorologiques, Toulouse) and Juliette Blanchet (Institut des Géosciences de l'Environnement, Grenoble) for their fruitful discussions on the project.

References

Ali, E., Cramer, W., Carnicer, J., Georgopoulou, E., Hilmi, N., Cozannet, G. L., & Piero, L. (2022). Cross-chapter paper 4: Mediterranean region. *Climate Change 2022: Impacts, Adaptation and Vulnerability*, 2233–2272. https://doi.org/10.1017/9781009325844.021

Allen, M. R., & Ingram, W. J. (2002). Constraints on future changes in climate and the hydrologic cycle. *Nature*, *419*(6903), 224–232. https://doi.org/10.1038/nature01092

Alpert, P., Ben-Gai, T., Baharad, A., Benjamini, Y., Yekutieli, D., Colacino, M., et al. (2002). The paradoxical increase of Mediterranean extreme daily rainfall in spite of decrease in total values. *Geophysical Research Letters*, *29*(11), 311–314. https://doi.org/10.1029/2001GL013554

Ambrosino, C., & Chandler, R. E. (2013). A nonparametric approach to the removal of documented inhomogeneities in climate time series. *Journal of Applied Meteorology and Climatology*, *52*(5), 1139–1146. https://doi.org/10.1175/jamc-d-12-0166.1

Azzopardi, B., Balzan, M. V., Cherif, S., Doblas-Miranda, E., dos Santos, M., Dobrinski, P., et al. (2020). Climate and environmental change in the mediterranean basin–current situation and risks for the future. *First Mediterranean assessment report*.

Bandhauer, M., Isotta, F., Lakatos, M., Lussana, C., Båserud, L., Izsák, B., et al. (2022). Evaluation of daily precipitation analyses in e-obs (v19. 0e) and era5 by comparison to regional high-resolution datasets in European regions. *International Journal of Climatology*, *42*(2), 727–747. https://doi.org/10.1002/joc.7269

Benestad, R. E., Parding, K. M., Erlandsen, H. B., & Mezghani, A. (2019). A simple equation to study changes in rainfall statistics. *Environmental Research Letters*, *14*(8), 084017. https://doi.org/10.1088/1748-9326/ab2bb2

Ben-Gai, T., Bitan, A., Manes, A., Alpert, P., & Rubin, S. (1998). Spatial and temporal changes in rainfall frequency distribution patterns in Israel. *Theoretical and Applied Climatology*, *61*(3–4), 177–190. https://doi.org/10.1007/s007040050062

Berthou, S., Kendon, E. J., Chan, S. C., Ban, N., Leutwyler, D., Schär, C., & Fosser, G. (2020). Pan-European climate at convection-permitting scale: A model intercomparison study. *Climate Dynamics*, *55*(1), 35–59. https://doi.org/10.1007/s00382-018-4114-6

Berthou, S., Rowell, D. P., Kendon, E. J., Roberts, M. J., Stratton, R. A., Crook, J. A., & Wilcox, C. (2019). Improved climatological precipitation characteristics over West Africa at convection-permitting scales. *Climate Dynamics*, *53*(3–4), 1991–2011. https://doi.org/10.1007/s00382-019-04759-4

Boberg, F., Berg, P., Thejll, P., Gutowski, W. J., & Christensen, J. H. (2010). Improved confidence in climate change projections of precipitation further evaluated using daily statistics from ENSEMBLES models. *Climate Dynamics*, *35*(7), 1509–1520. https://doi.org/10.1007/s00382-009-0683-8

Brunetti, M., Buffoni, L., Maugeri, M., & Nanni, T. (2000). Precipitation intensity trends in Northern Italy. *International Journal of Climatology*, *20*(9), 1017–1031. https://doi.org/10.1002/1097-0088(200007)20:9{<}1017::AID-JOC515{>}3.0.CO;2-S

Brunetti, M., Maugeri, M., Monti, F., & Nanni, T. (2004). Changes in daily precipitation frequency and distribution in Italy over the last 120 years. *Journal of Geophysical Research*, *109*(D5), D05102. https://doi.org/10.1029/2003JD004296

Caloiero, T., Caloiero, P., & Frustaci, F. (2018). Long-term precipitation trend analysis in Europe and in the Mediterranean basin. *Water and Environment Journal*, *32*(3), 433–445. https://doi.org/10.1111/wej.12346

Chinita, M. J., Richardson, M., Teixeira, J., & Miranda, P. M. (2021). Global mean frequency increases of daily and sub-daily heavy precipitation in era5. *Environmental Research Letters*, *16*(7), 074035. https://doi.org/10.1088/1748-9326/ac0caa

Coles, S., Bawa, J., Trenner, L., & Dorazio, P. (2001). *An introduction to statistical modeling of extreme values* (Vol. 208). Springer.

Colin, J. (2011). *Etude des événements précipitants intenses en Méditerranée: Approche par la modélisation climatique régionale (Unpublished doctoral dissertation)*. Université de Toulouse, Université Toulouse III—Paul Sabatier.

Cornes, R., Schrier, G., Van den Besselaar, E., & Jones, P. (2018). An ensemble version of the E-OBS temperature and precipitation data sets. *Journal of Geophysical Research: Atmospheres*, *123*(17), 9391–9409. https://doi.org/10.1029/2017JD028200

D'Agostino, R., & Lionello, P. (2020). The atmospheric moisture budget in the Mediterranean: Mechanisms for seasonal changes in the Last Glacial Maximum and future warming scenario. *Quaternary Science Reviews*, *241*, 106392. https://doi.org/10.1016/j.quascirev.2020.106392

Drobinski, P., Da Silva, N., Bastin, S., Mailler, S., Muller, C., Ahrens, B., et al. (2020). How warmer and drier will the Mediterranean region be at the end of the twenty-first century? *Regional Environmental Change*, *20*(3), 12. https://doi.org/10.1007/s10113-020-01659-w

Drobinski, P., Silva, N. D., Panthou, G., Bastin, S., Muller, C., Ahrens, B., et al. (2018). Scaling precipitation extremes with temperature in the Mediterranean: Past climate assessment and projection in anthropogenic scenarios. *Climate Dynamics*, *51*(3), 21–1257. https://doi.org/10.1007/s00382-016-3083-x

Ferguson, C. R., & Villarini, G. (2012). Detecting Inhomogeneities in the twentieth century reanalysis over the central United States. *Journal of Geophysical Research*, *117*(D5), D05123. https://doi.org/10.1029/2011jd016988

Fischer, E. M., Beyerle, U., & Knutti, R. (2013). Robust spatially aggregated projections of climate extremes. *Nature Climate Change*, *3*(12), 1033–1038. https://doi.org/10.1038/nclimate2051

Fischer, E. M., & Knutti, R. (2014). Detection of spatially aggregated changes in temperature and precipitation extremes. *Geophysical Research Letters*, *41*(2), 547–554. https://doi.org/10.1002/2013gl058499

Giorgi, F. (2006). Climate change hot-spots. *Geophysical Research Letters*, *33*(8), L08707. https://doi.org/10.1029/2006gl025734

Giorgi, F., Coppola, E., Raffaele, F., Diro, G. T., Fuentes-Franco, R., Giuliani, G., et al. (2014). Changes in extremes and hydroclimatic regimes in the crema ensemble projections. *Climatic Change*, *125*(1), 39–51. https://doi.org/10.1007/s10584-014-1117-0

Groisman, P. Y., Karl, T. R., Easterling, D. R., Knight, R. W., Jamason, P. F., Hennessy, K. J., et al. (1999). Changes in the probability of heavy precipitation: Important indicators of climatic change. *Weather and Climate Extremes: changes, variations and a perspective from the insurance industry*, 243–283. https://doi.org/10.1007/978-94-015-9265-9_15

Held, I. M., & Soden, B. J. (2006). Robust responses of the hydrological cycle to global warming. *Journal of Climate*, *19*(21), 5686–5699. https://doi.org/10.1175/JCLI3990.1

Hersbach, H., Bell, B., Berrisford, P., Biavati, G., Horányi, A., Muñoz Sabater, J., et al. (2018). Era5 hourly data on single levels from 1959 to present [Dataset]. *Copernicus climate change service (c3s) Climate Data Store (cds)*. https://doi.org/10.24381/cds.adbb2d47

Hersbach, H., Bell, B., Berrisford, P., Hirahara, S., Horányi, A., Muñoz-Sabater, J., et al. (2020). The ERA5 global reanalysis. *Quarterly Journal of the Royal Meteorological Society*, *146*(730), 1999–2049. https://doi.org/10.1002/qj.3803

Hoerling, M., Eischeid, J., Perlwitz, J., Quan, X., Zhang, T., & Pegion, P. (2012). On the increased frequency of mediterranean drought. *Journal of Climate*, *25*(6), 2146–2161. https://doi.org/10.1175/JCLI-D-11-00296.1

Intergovernmental Panel On Climate Change. (2023). *Climate change 2021 – the physical science basis: Working group I contribution to the sixth assessment report of the intergovernmental Panel on climate change* (1st Ed.). Cambridge University Press. https://doi.org/10.1017/9781009157896

Karl, T. R., Nicholls, N., & Ghazi, A. (1999). Clivar/gcos/wmo workshop on indices and indicators for climate extremes workshop summary. *Weather and Climate Extremes: Changes, variations and a perspective from the insurance industry*, 3–7. https://doi.org/10.1007/978-94-015-9265-9_2

Kistler, R., Kalnay, E., Collins, W., Saha, S., White, G., Woollen, J., et al. (2001). The ncep–ncar 50-year reanalysis: Monthly means cd-rom and documentation. *Bulletin of the American Meteorological Society*, *82*(2), 247–268. https://doi.org/10.1175/1520-0477(2001)082<0247:tnnyrm>2.3.co;2

Klingaman, N. P., Martin, G. M., & Moise, A. (2017). ASoP (v1.0): A set of methods for analyzing scales of precipitation in general circulation models. *Geoscientific Model Development*, *10*(1), 57–83. https://doi.org/10.5194/gmd-10-57-2017

Krueger, O., Schenk, F., Feser, F., & Weisse, R. (2013). Inconsistencies between long-term trends in storminess derived from the 20cr reanalysis and observations. *Journal of Climate*, *26*(3), 868–874. https://doi.org/10.1175/jcli-d-12-00309.1

Mariotti, A., Pan, Y., Zeng, N., & Alessandri, A. (2015). Long-term climate change in the Mediterranean region in the midst of decadal variability. *Climate Dynamics*, *44*(5–6), 20–1456. https://doi.org/10.1007/s00382-015-2487-3

Myhre, G., Alterskjær, K., Stjern, C. W., Hodnebrog, Ø., Marelle, L., Samset, B. H., et al. (2019). Frequency of extreme precipitation increases extensively with event rareness under global warming. *Scientific Reports*, *9*(1), 16063. https://doi.org/10.1038/s41598-019-52277-4

Naveau, P., Huser, R., Ribereau, P., & Hannart, A. (2016). Modeling jointly low, moderate, and heavy rainfall intensities without a threshold selection. *Water Resources Research*, *52*(4), 2753–2769. https://doi.org/10.1002/2015WR018552

Peña-Angulo, D., Vicente-Serrano, S. M., Domínguez-Castro, F., Murphy, C., Reig, F., Tramblay, Y., et al. (2020). Long-term precipitation in Southwestern Europe reveals no clear trend attributable to anthropogenic forcing. *Environmental Research Letters*, *15*(9), 094070. https://doi.org/10.1088/1748-9326/ab9c4f

Pendergrass, A. G., & Hartmann, D. L. (2014). The atmospheric energy constraint on global-mean precipitation change. *Journal of Climate*, *27*(2), 757–768. https://doi.org/10.1175/jcli-d-13-00163.1

Pfahl, S., O'Gorman, P. A., & Fischer, E. M. (2017). Understanding the regional pattern of projected future changes in extreme precipitation. *Nature Climate Change*, *7*(6), 423–427. https://doi.org/10.1038/nclimate3287

Pichelli, E., Coppola, E., Sobolowski, S., Ban, N., Giorgi, F., Stocchi, P., et al. (2021). The first multi-model ensemble of regional climate simulations at kilometer-scale resolution part 2: Historical and future simulations of precipitation. *Climate Dynamics*, *56*(11), 3581–3602. https://doi.org/10.1007/s00382-021-05657-4

Pierce, D. W., Cayan, D. R., Das, T., Maurer, E. P., Miller, N. L., Bao, Y., et al. (2013). The key role of heavy precipitation events in climate model disagreements of future annual precipitation changes in California. *Journal of Climate*, *26*(16), 5879–5896. https://doi.org/10.1175/JCLI-D-12-00766.1

Pohlmann, H., & Greatbatch, R. J. (2006). Discontinuities in the late 1960's in different atmospheric data products. *Geophysical Research Letters*, *33*(22), L22803. https://doi.org/10.1029/2006gl027644

Polade, S. D., Pierce, D. W., Cayan, D. R., Gershunov, A., & Dettinger, M. D. (2014). The key role of dry days in changing regional climate and precipitation regimes. *Scientific Reports*, *4*(1), 4364. https://doi.org/10.1038/srep04364

Raymond, F., Ullmann, A., Camberlin, P., Drobinski, P., & Smith, C. C. (2016). Extreme dry spell detection and climatology over the Mediterranean Basin during the wet season. *Geophysical Research Letters*, *43*(13), 9–7204. https://doi.org/10.1002/2016GL069758

Reid, M. (2022). Reliability – A python library for reliability engineering [Computer software manual]. *Zenodo*. https://doi.org/10.5281/zenodo.3938000

Rivoire, P., Le Gall, P., Favre, A.-C., Naveau, P., & Martius, O. (2022). High return level estimates of daily era-5 precipitation in Europe estimated using regionalized extreme value distributions. *Weather and Climate Extremes*, *38*, 100500. https://doi.org/10.1016/j.wace.2022.100500

Rivoire, P., Martius, O., & Naveau, P. (2021). A comparison of moderate and extreme ERA-5 daily precipitation with two observational data sets. *Earth and Space Science*, *8*(4), e2020EA001633. https://doi.org/10.1029/2020EA001633

Schär, C., Ban, N., Fischer, E. M., Rajczak, J., Schmidli, J., Frei, C., et al. (2016). Percentile indices for assessing changes in heavy precipitation events. *Climatic Change*, *137*(1), 201–216. https://doi.org/10.1007/s10584-016-1669-2

Shangguan, M., Wang, W., & Jin, S. (2019). Variability of temperature and ozone in the upper troposphere and lower stratosphere from multi-satellite observations and reanalysis data. *Atmospheric Chemistry and Physics*, *19*(10), 6659–6679. https://doi.org/10.5194/acp-19-6659-2019

Sheffield, J., & Wood, E. F. (2012). *Drought: Past problems and future scenarios*. Routledge.

Sousa, P. M., Trigo, R. M., Aizpurua, P., Nieto, R., Gimeno, L., & García Herrera, R. (2011). Trends and extremes of drought indices throughout the 20th century in the Mediterranean. *Natural Hazards and Earth System Sciences*, *11*(1), 19–51. https://doi.org/10.5194/nhess-11-33-2011

Tanarhte, M., Hadjinicolaou, P., & Lelieveld, J. (2012). Intercomparison of temperature and precipitation data sets based on observations in the mediterranean and the Middle East. *Journal of Geophysical Research*, *117*(D12), D12102. https://doi.org/10.1029/2011jd017293

Taszarek, M., Allen, J. T., Marchio, M., & Brooks, H. E. (2021a). Global climatology and trends in convective environments from era5 and rawinsonde data. *NPJ climate and atmospheric science*, *4*(1), 35. https://doi.org/10.1038/s41612-021-00190-x

Taszarek, M., Pilguj, N., Allen, J. T., Gensini, V., Brooks, H. E., & Szuster, P. (2021b). Comparison of convective parameters derived from era5 and merra-2 with rawinsonde data over Europe and North America. *Journal of Climate*, *34*(8), 3211–3237. https://doi.org/10.1175/jcli-d-20-0484.1

Tencaliec, P., Favre, A.-C., Naveau, P., Prieur, C., & Nicolet, G. (2020). Flexible semiparametric generalized Pareto modeling of the entire range of rainfall amount. *Environmetrics*, *31*(2), e2582. https://doi.org/10.1002/env.2582

Trenberth, K. E. (1999). Conceptual framework for changes of extremes of the hydrological cycle with climate change. *Climatic Change*, *42*(1), 327–339. https://doi.org/10.1023/A:1005488920935

Trenberth, K. E. (2011). Changes in precipitation with climate change. *Climate Research*, *47*(1–2), 123–138. https://doi.org/10.3354/cr00953

Urdiales-Flores, D., Zittis, G., Hadjinicolaou, P., Osipov, S., Klingmüller, K., Mihalopoulos, N., et al. (2023). Drivers of accelerated warming in mediterranean climate-type regions. *npj Climate and Atmospheric Science*, *6*(1), 97. https://doi.org/10.1038/s41612-023-00423-1

Vautard, R., Gobiet, A., Sobolowski, S., Kjellström, E., Stegehuis, A., Watkiss, P., et al. (2014). The European climate under a 2°C global warming. *Environmental Research Letters*, *9*(3), 12. https://doi.org/10.1088/1748-9326/9/3/034006

Zhang, X., Alexander, L., Hegerl, G. C., Jones, P., Tank, A. K., Peterson, T. C., et al. (2011). Indices for monitoring changes in extremes based on daily temperature and precipitation data. *WIREs Climate Change*, *2*(6), 851–870. https://doi.org/10.1002/wcc.147

Zittis, G. (2018). Observed rainfall trends and precipitation uncertainty in the Vicinity of the Mediterranean, Middle East and North Africa. *Theoretical and Applied Climatology*, *134*(3), 1207–1230. https://doi.org/10.1007/s00704-017-2333-0

Zittis, G., Bruggeman, A., & Lelieveld, J. (2021). Revisiting future extreme precipitation trends in the mediterranean. *Weather and Climate Extremes*, *34*, 100380. https://doi.org/10.1016/j.wace.2021.100380